Applied Thermal Engineering xxx (2014) 1–18

Contents lists available at ScienceDirect

Applied Thermal Engineering

journal homepage: www.elsevier.com/locate/apthermeng

The role of enhancement techniques on heat and mass transfer characteristics of shell and tube spray evaporator: a detailed review

Azher M. Abed [a, b, **], M.A. Alghoul [a, *], Mohammad H. Yazdi [a], Ali Najah Al-Shamani [a], K. Sopian [a]

[a] Solar Energy Research Institute, Universiti Kebangsaan Malaysia (UKM), 43600 Bangi, Selangor, Malaysia
[b] Department of Air Conditioning and Refrigeration, Al-Mustaqbal University College, Babylon, Iraq

HIGHLIGHTS

- Heat and mass transfer of shell and tube spray evaporators are still subjective for further enhancement.
- The advantage of spray cooling is its capability of additional heat removal.
- Highlight the key areas, which need attention such as enhancement techniques and falling film flow.
- Traditional heat transfer fluids have inherently poor thermal conductivities.
- Combining advanced and new technologies together can enhance functions and properties.

ARTICLE INFO

Article history:
Received 9 March 2014
Accepted 9 October 2014
Available online xxx

Keywords:
Shell and tube evaporator
Falling film flow
Enhancement techniques
Heat & mass transfer characteristics
Efficiency–compactness–cost

ABSTRACT

Falling film heat transfer of horizontal shell-side evaporators remains of interest to scientists due to the complexity of these phenomena for practical applications. However, characteristics of heat and mass transfers of spray evaporators are still subject to further enhancement. This study is to review the enhancement techniques and falling film flow especially the effect of nanoparticles suspended with refrigerants in order to confirm their role. The study covers the influence of surface geometry (bundles and external of tubes), normal single tube, low fins, and enhanced geometrical tubes; effect of additives; and the applications and problems related to refrigerant-based nanofluids. Heat transfer area with energy related cost and the significant efforts on empirical correlations for heat transfer coefficient are discussed. It is found that the interaction of the heat and mass transfer process on falling film flow and contradictions of thermal physical properties of nanofluids should all be taken into careful consideration. In addition, existing research on both heat and mass transfer regarding nanofluids are found to be inadequate, and still requires extensive experimental and theoretical work on their salient parameters. Finally, this study highlights the factors affecting efficiency, compactness, and cost of the spray evaporator and the potential of enhancement techniques.

1. Introduction

In industrial settings, falling-film evaporators can substitute flooded evaporators in refrigeration systems, as its use is widespread, owing to its high solution side heat transfer coefficient, and its rather minuscule liquid inventory as opposed to flooded evaporators. Despite the fact that evaporators of this form was initially patented in 1888 [1], there were only a small number of researchers that were seriously working on it prior to the 1970s. Since then, many investigators have studied this technology; however, the work during the 1970s emphasized the utilization of falling-film evaporators for ocean thermal energy conversion (OTEC) systems, and this field was revived in the 1980s due to the second world oil crisis. The working fluid used was water, or ammonia in the case of (OTEC). The phasing out of CFC in the 1990s prompted a more widespread usage of falling-film evaporators. Despite the obvious advantages vis-à-vis refrigeration and air-conditioning, falling-film evaporators are not widely used for both applications. The reluctance of utilizing this technology is due to the complications in disseminating liquids in a uniform

* Corresponding author. Tel.: +60 192618126.
** Corresponding author. Solar Energy Research Institute, Universiti Kebangsaan Malaysia (UKM), 43600 Bangi, Selangor, Malaysia.
E-mail addresses: azhermuhson@gmail.com (A.M. Abed), dr.alghoul@gmail.com (M.A. Alghoul).

http://dx.doi.org/10.1016/j.applthermaleng.2014.10.020
1359-4311/

Nomenclature

C_P	specific heat, (J/kg K)
Do	outside diameter, (m)
dp	nanoparticle diameter, (nm)
g	gravitational acceleration, (m/s)
Ga	modified Galileo number or (kaptiza number), $(\rho^*\sigma^3/\mu^4{}^*g)$
H	liquid feeder height, (m)
h	heat transfer coefficient, (W/m^2 K)
k	thermal conductivity, (W/m K)
Nu	Nusselt number, $(h/k_l)(\nu_l^2/g)^{1/3}$, dimensionless
p	pressure, (N/m^2)
Pr	Prandtl number, $k/\rho C_P$, dimensionless
Re	Reynolds number
T	temperature

Greek letters

α	pool boiling heat transfer coefficient, (W/m^2 K)
$Ø$	concentration ratio of nanofluids
Γ	liquid mass flow rate per unit length of tube (each side), (kg/m s)
μ	dynamic viscosity, (kg/m s)
ν	kinematic viscosity, (m^2/s)
ρ	density, (kg/m^3)
σ	surface tension, (kg/s^2)
ξ	capillary constant given by $[\sigma/\rho_l{}^*g]^{1/2}$, (m)

Subscripts

crit	referred to the critical state
l	liquid
sat	saturation
v	vapor

manner over a surface of a tube array to form thin films that are suitable for evaporative heat transfers. This renders process optimization of this system for the purpose of evaporation extremely difficult. Also, the optimization of falling-film heat exchanger requires a detailed comprehension of both the influence of wall superheat and solution sub-cooling on the ratio of evaporation-to-sensible heat transfer. Evaporation heat transfer is still a relevant and challenging research topic, despite the fact that intense work on this area has been ongoing for decades. Thome [2] and Ribatskia and Jacob [3] focused on studies published from 1994 to 2005. Recently, Fernández-Seara and Pardiñas [4] focused mainly on heat transfer and fluid dynamics of falling film evaporation and to the best of our knowledge, only a few data is present in literature on falling-film heat and mass transfers. This paper reviews the literature on horizontal-tube and falling-film-type evaporators, with special emphasis on defining the characteristics of both heat and mass transfers of falling-film evaporators under different enhancement techniques. Furthermore, other factors, including pressure losses and cost effects, are studied as well.

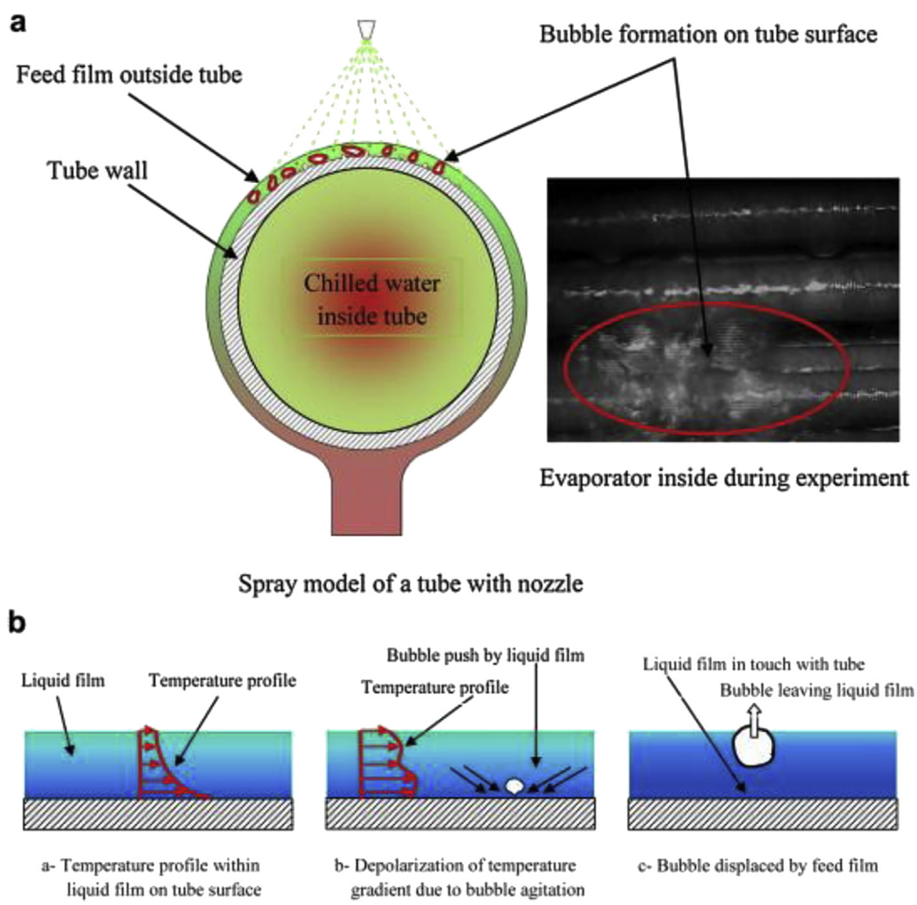

Fig. 1. (a) Bubble formation on tube surface and spray model. (b) Bubble agitation in liquid film [6].

Please cite this article in press as: A.M. Abed, et al., The role of enhancement techniques on heat and mass transfer characteristics of shell and tube spray evaporator: a detailed review, Applied Thermal Engineering (2014), http://dx.doi.org/10.1016/j.applthermaleng.2014.10.020

2. Falling film evaporation concept

Falling film evaporation is controlled by two different heat transfer processes. The thin film evaporation is a heat transfer mechanism controlled by conduction and convection across the film, where phase change occurs at the interface, and whose magnitude is directly related to the thickness of the film, and the form of the film. Increasing the heat flux will initiate the boiling of the nucleates; and the bubbles of vapors expands and moves along the films in tandem with the flow in a way that will allow both thin falling-film evaporation and nucleate boiling to be poignant in heat transfer, as it is dependent on both heat flux and liquid mass flow rates [3,5]. Instability mechanisms are vital to the evaporation of falling films. Viscosity, gravity, and surface tension effects usually dominate liquid film flows. The circumstances may give rise to interfacial waves on the thin liquid film that might strongly affect the vaporization rate by increasing the interfacial area and enhancing the convective transport near the interface [6]. Fig. 1 shows the spray profile and evaporation phenomena on the liquid film of flow boiling. It is also known that there are three distinct regime that are discernable from spray cooling heat transfer [7]; a low temperature regime where the liquid evaporates at the free liquid–vapor interface, a high temperature regime where liquid films are in a film-boiling-like state, and vapor bubbles are generated at the superheated hot wall. The third regime is the transition from the low temperature to the high temperature region.

3. Effect of surface geometry on falling film evaporator

3.1. Overview on shell and tube evaporator

Shell-and-tube evaporators are widely used in chillers, industrial refrigeration, and heat pumping applications. In refrigeration systems, the evaporator cools the fluids (liquid or air). The refrigerant is only there to absorb the energy of the fluid that we want cooled, which result in the refrigerant being boiled. The classification of refrigeration evaporators are conducted as per the liquid feed method being used, in the form of direct-expansion evaporators, flooded evaporators, and overfeed evaporators. An expansion valve fills the direct expansion evaporators, which functions as a regulator of liquid flow that passes through the evaporator. The working concept of a flooded evaporator involves completely filling it with a liquid refrigerant to wet the internal exposed surface, which will improve its heat transfer coefficient. Some examples are discussed in Refs. [8–14]. Horizontal-tube falling film evaporators belong to typical overfeed evaporators. Falling film evaporators seems to be a viable replacement for both air-conditioning and refrigerating applications, due to their higher cycle efficiency, lower costs, and negligible environmental impact, owing to its reduced refrigerant charges (e.g. the overall refrigerant inventory decrease along with the penalty [15]), enhanced heat transfer (e.g. Zeng et al. [16] in their results found that the spray evaporation coefficient is 65% higher than the flooded boiling bundle), minimizing the evaporator's size (e.g. Ayub et al. [17] in their design of spray evaporator, was a half-bundle shell and tube configuration). A number of studies related to the effects of the falling film evaporator in refrigeration systems have increased in the last few years. Their studies indicated that the spray evaporators are superior to flooded evaporators when employed in heat transfer applications [18–22]. The advantage of spray cooling is its capability of additional heat removal, mostly by impacting droplets and surface renewal effects, which is highly beneficial in both boiling and non-boiling regimes. There has been quite a number of works being done on the experimental, analytical, and numerical aspects of sprays and spray cooling over the past decades, mostly in the quest to comprehend the basic mechanisms of sprays and spray cooling behavior, e.g. Refs. [23–31]. Moreover, there are various parameters that affect the performance of shell and tube evaporators, and these were determined by numerous experimental and theoretical investigations [32–39] designed to understand the characteristics and behaviors of shell and tube evaporators. The influence of spray parameters upon its ability to remove heat has formed the topic of many researches over the years. Zeng et al. [16,20,22,40] analyzed the effects of heat flux, saturation temperature, spray flow rate, nozzle height, and nozzle type (standard angle or wide-angle) with a 3-2-3 triangular. The results showed lower heat transfer coefficients with wide-angle nozzles, as shown in Fig. 2a. It was concluded that in spray evaporation via spray nozzle, the effect of tube bundles are less pronounced at reduced saturation temperatures, low spray flow rate, minuscule nozzle heights, or standard angles, as opposed to wide-angled nozzles, displayed in Fig. 2b and c.

Chang et al. [19] analyzed the performance of triangular-pitch shell-and-tube evaporators from the perspective of heat transfer via an interior spray technique. It was determined that the heat transfer performance for this type of spray evaporator system is better than that obtained using a pool boiling type system. As a matter of fact, it is quite difficult to realize a uniform, all-encompassing distribution, which will in turn influence flow and drying, more so in deep setting bundles, as shown in Fig. 3.

The heat transfer enhancement achieved by the effect of liquid sprays impact is associated with the heat flux at different inclination angles, and in Refs. [41,42], their results showed that the maximum critical heat flux (CHF) was always realized with spray impinging normal to the test surface; increasing angle of inclination away from the normal decreased CHF appreciably. Lin et al. [43] analyzed the influence of the spray axis's incident angle (0°, 45°, 60° and 75°) upon the performance of heat transfer of a rhombus-pitch shell-and-tube interior spray evaporator. The optimum heat transfer was achieved at an incident angle that was slightly lower than 60°, shown in Fig. 4. It is rather obvious that the spray cooling method is far superior in terms of heat transfer at all values.

3.2. Single horizontal tube and smooth tube

Generally, studies involving smooth tubes encompass parameters such as heat flux and flow rates. The film's thickness distribution and average thickness outside a horizontal tube has already been measured by numerous investigators [44–48]. The results showed that circumferential angle, intertube spacing, and the film's Reynolds number mainly affect the distribution characteristics of the film's thickness. Based on the experimental data of Hou et al. [47], a new correlation has been suggested to predict the film's thickness. The correlation results and the corresponding standard deviation are shown in Table 1.

$$\delta = c\left(\frac{3\mu_L \Gamma}{\rho_L(\rho_L - \rho_G) g \sin\beta}\right)^{1/3}\left(\frac{S}{D}\right)^n \tag{1}$$

It should also be pointed out that heat transfer coefficients are almost independent of flow rates in the context of convection-dominated conditions [46,49], while it increases with $\boldsymbol{\Gamma}$ [50], and also increases with an increase in the distributor's height, reduction of piping diameters, increase of the evaporation boiling point, and the reduction of the total temperature difference Δt [46]. Furthermore, increasing flow rates increases the heat transfer coefficients after a certain minimum value has been achieved [51]. This critical value might be representative of a transition phase from laminar-to-turbulent film flows [52]. Mohamed [53] examined the effect

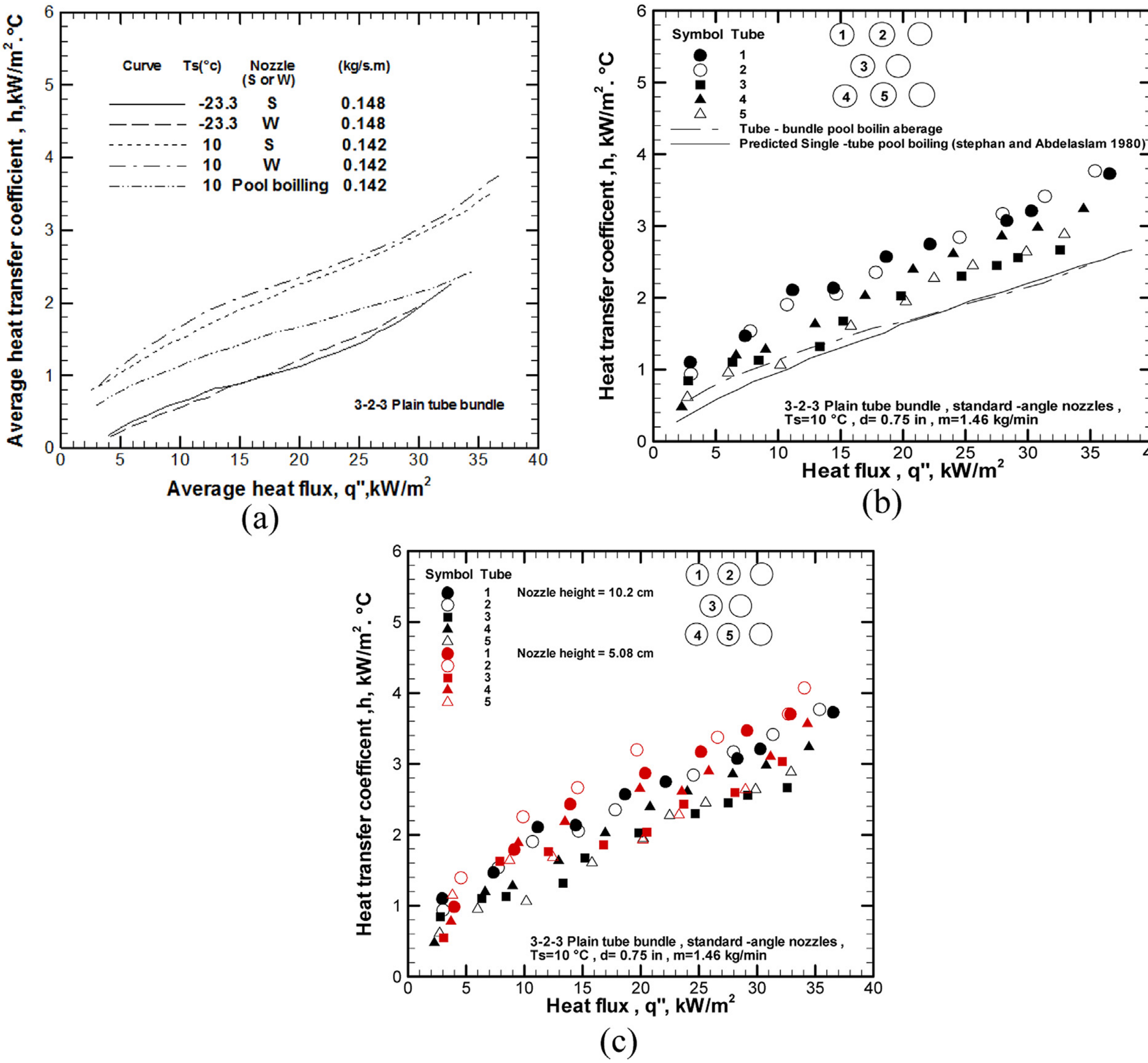

Fig. 2. Spray evaporation performance for: a) standard nozzle and wide nozzle at $d = (0.75$ inch) with pool billing. b) Tube bundle at nozzle height of 10.2 cm and c) tube bundle with different nozzle heights [16,40].

of rotational speed of the tube on the horizontal falling-film behavior. The flow mode transitions, film's thickness, and the film's wavelength were studied as well. It is recommended that the tube speed of rotation not exceed the maximum speed of rotation, which might result in an unstable falling-film. At least two works suggested a tube-spacing effect on the mode transitions [54,55], and highly simplified the thermodynamic analysis to predict the transitions between falling-film modes. The simplified analysis of interfacial energy result in a new scaling relationship for the transitional Reynolds numbers for all the falling-film mode transitions, and was found to be $Re = Ga^{1/4}\sqrt{S/\xi}$. The effects of viscous pure liquids on falling-film evaporating were studied by Weise and Scholl [56], and their results showed a significant enhancement in wave development due to the film's distribution. They discovered that nucleate boiling could be allowed without causing film instabilities over a significant range of wall superheating.

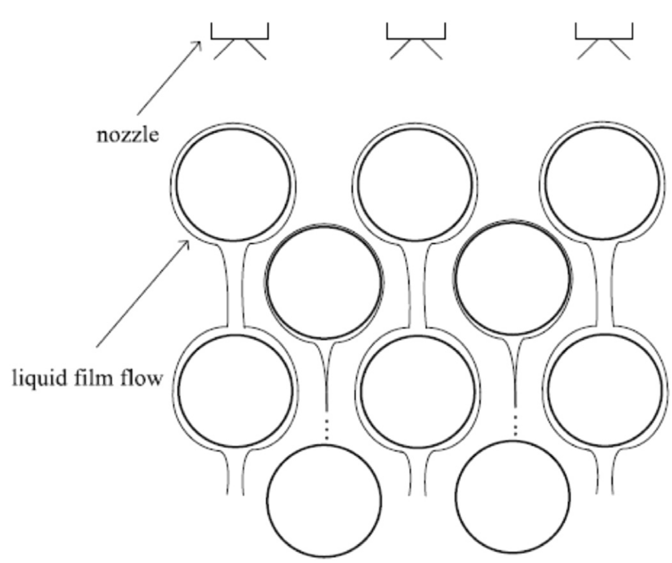

Fig. 3. Liquid film distribution in triangular-pitch tube with spray nozzle by Chang et al. [19].

3.3. Finned and enhanced tube surface

The utilization of passive techniques can improve heat transfer by a factor of 10 compared to those on plain surfaces. Finned

Please cite this article in press as: A.M. Abed, et al., The role of enhancement techniques on heat and mass transfer characteristics of shell and tube spray evaporator: a detailed review, Applied Thermal Engineering (2014), http://dx.doi.org/10.1016/j.applthermaleng.2014.10.020

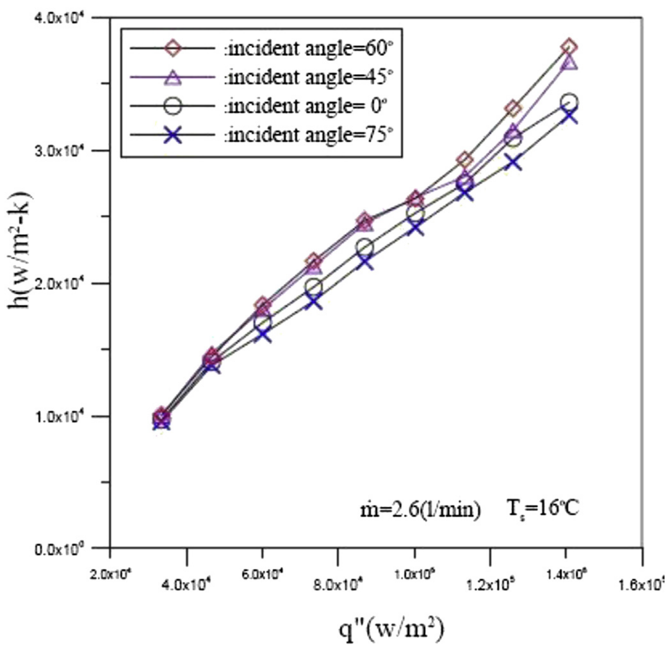

Fig. 4. Variation of heat transfer coefficient with surface heat flux as function of spray incident angle (0°, 45°, 60° and 75°) for spray rate of 2.6 l/min and saturation temperature of T_{sat} = 16 °C [43].

Table 1
Correlation of measured film thickness [47].

β (°)	C	n	D (mm)	SD
$0° < \beta \leq 90°$	0.97540	−0.16670	25.4	0.0987
$90° < \beta \leq 180°$	0.84978	−0.16479	25.4	0.0627

surfaces can also improve the performance of plain tubes. To improve the performance of falling-film, the artificially formed sits must be conducive to nucleate boiling at lower temperature differences, increase internal turbulence of the films, and enhance the heat transfer area. One of the earliest work on enhanced heat transfer for spray evaporation of ammonia was by Zeng et al. [57], who analyzed the ammonia spray evaporation heat transfer performance of single low-fin and corrugated tubes. It was proven that the heat transfer coefficient of spray evaporation is higher by a factor of 2.8 compared to its counterpart with single plain tube under spray conditions, as shown in Fig. 5. The predictive methods for pool boiling heat transfer coefficient (α) available in the literature at present are empirical or semi empirical, especially for heat transfer conditions relevant in practice. The heat transfer coefficient is proportional to Aq^n. The boiling heat transfer coefficients were obtained by the Wilson-plot technique. This correlation has been fitted to experimental data near the atmospheric pressure. The uncertainty of the heat transfer coefficient was given to ±13%. The heat transfer coefficients primarily increase with heat flux (8–60 kW/m^2) and saturation temperature (−23.3 to +10 °C). It was shown that the pool boiling heat transfer coefficient increase from (500–2000 W/m^2 K), while the heat transfer coefficient of spray evaporation increase from (1000–5000 W/m^2 K) at all saturation temperatures.

Garcia et al. [58] conducted an experimental and numerical study of small capacity ammonia shell and tube evaporator with external low fin tubes. The results showed that the traditional smooth tube shell and tube evaporators are still quite ubiquitous in ammonia applications in developing countries. Silk et al. [59] analyzed the influence of both improved surfaces and spray inclination angles. The surface enhancements consisted of cubic pin fins, pyramids, and straight fins, while PF-5060 was the working fluid. The results proved that the straight finned surface demonstrated the best performance, and spray angles exceeding 15° removed any liquid remaining on the heater's surface, mostly due the multinozzle array stagnation zone phenomena. Ayub [60] presented an overview of improved heat transfer in ammonia systems and future trends in the development of compact heat exchangers for ammonia refrigeration. The proposal involved the usage of multiple types of tubes with high efficiencies for an ammonia spray evaporator. Oliet et al. [35] presented a novel model of fin-and-tube evaporators in the context of non-uniform in-tube heat transfer. A single-tube heat exchanger was selected as a representative of an ammonia liquid

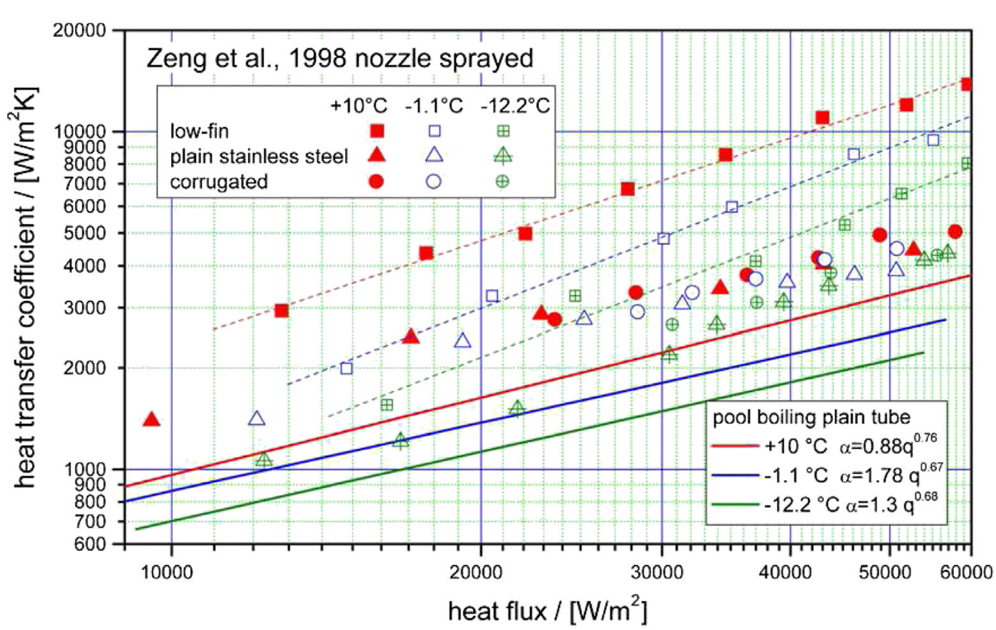

Fig. 5. Heat transfer enhancement by nozzle spray evaporation on a plain, low-fin and corrugated tube [57].

overfeed evaporator in order to demonstrate the capabilities of the model in determining the fin, tube, and in-tube refrigerant local conditions. Enhanced tube heat exchangers with pool boiling evaporator were used for ammonia and other fluids for the purpose of redacting the refrigerant's inventory of the plant. Christians and Thome [61,62] tested falling film evaporation of different enhanced tubes. Two enhanced boiling tubes, the Wolverine Turbo-B5 and the Wieland Gewa-B5, were tested using R-134a and R-236fa, and it was determined that the R-134a outperformed R-236fa in the context of refrigerants.

3.4. Structured enhanced surface

Surfaces that are structured are conducive to nucleate boiling in films at reasonable temperature differences, enhance internal film turbulence, while also increasing the area viable for heat transfer. Putilin et al. [63] analyzed the mechanisms of heat transfer of flowing liquids that are moving downwards from horizontal and profiled tubes. Liu and Yi [64–66] carried out an experimental study for the enhancement of falling film evaporation heat transfer of pure water, water/salt mixtures, and R11 across horizontal smooth tubes and two kinds of structured tube bundles under atmospheric pressure. The results showed that the low-cost roll-worked tube can greatly enhance the evaporation heat transfer performance of the falling film, and make it comparable to those of expensive commercial enhanced tubes, such as GEWA-T tubes; TE tubes and HF tubes even at low and moderate heat flux levels. Kim et al. [67] studied the evaporation in oval or flat tube with different aspect ratios using R-410A as its working fluid. The results showed that the evaporation heat transfer coefficient increases as mass flux,

a. Flattened smooth tubes having different aspect ratios

b. Both enhanced outer and inner surfaces

c. Fins on Turbo-CAB tubes

d. Low–fin carbon steel tube

e. Sturctured surface carbon steel tube .

f. A high ridge internal grovve with larger helix angle .

Fig. 6. Some enhanced surfaces for a low charge refrigerant.

Please cite this article in press as: A.M. Abed, et al., The role of enhancement techniques on heat and mass transfer characteristics of shell and tube spray evaporator: a detailed review, Applied Thermal Engineering (2014), http://dx.doi.org/10.1016/j.applthermaleng.2014.10.020

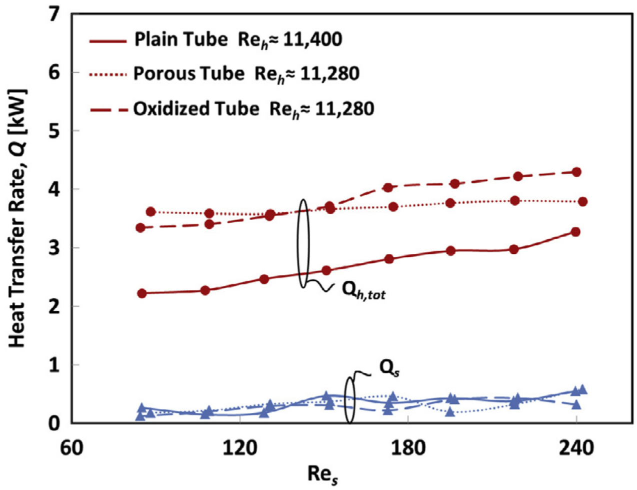

Fig. 7. Comparison of the overall heat transfer rates for the plain, oxidized, and porous-layer coated tubes tested in the evaporator [71].

heat flux, or saturation temperature increases, along with increasing aspect ratio.

Many techniques are employed for filling film on tubes, summarized in Fig. 6. The recently developed surfaces greatly enhance the filling film heat transfer, allowing the distribution of liquid refrigerant to occur at lower superheated wall, which ultimately reduced the physical size of these heat exchangers.

3.5. Porous enhanced surfaces

Certain models that predict porous falling film surfaces from the lack of film dimensions were proposed. Forrest et al. [68] analyzed the influence of nanoparticle thin-film coatings upon the augmentation of nucleate boiling heat transfer and critical heat fluxes. It was concluded that the nanoporous structure, coupled with the chemical constituency of these coatings, leads to enhanced boiling behavior. Wang et al. [69] carried out an experimental study on the mixing effect of falling film on coated division tube by the thermal tracing technique. The results showed that the convergent and accumulated liquid film at the coated division promoted better mixing, renewed liquid film interface, and further increased the liquid film side heat transfer efficiency. Lee et al. [70] analyzed the influence of a micro-scale porous layer coating on solution wetting and heat transfer of a horizontal-tube and falling-film heat exchanger. The results proved that the rate of heat transfer of the porous-layer coated tubes was higher by a factor of two compared to their plain tubes counterparts. Köroğlu et al. [71] studied the effect of copper oxidation in NaOH aqueous solutions by a chemical immersion method to create nano/micro-scale surface morphology on heat transfer surfaces and control their liquid wettability. The surface wetting and heat transfer performance of three different evaporators of plain (untreated), oxidized, and porous-layer coated tubes were compared. Fig. 7 compares the total heat transfer rates ($Q_{h,tot}$) with the sensible heat transfer rates (Q_s) of the tube arrays for the plain, oxidized, and porous-layer coated tubes. It was shown that among three different evaporators of plain (untreated), oxidized (in 0.1 M NaOH solution for 48 h), and porous-layer coated tubes, the oxidized tubes always demonstrated higher heat transfer rates than the plain tubes, and outperformed the porous-layer coated tubes for higher solution flow rates.

Köroğlu et al. [72] analyzed the influence of tube rows of sintered micro-scale porous-layer coating on both solution wetting and system-wide heat transfer, and surmised that performance can be doubled at minimum solution flow rates. It is assumed that this is caused by the spread of capillary-driven liquid and evaporation of thin films at the menisci on the coating. Recently, Bogan and Park [73] conducted an experimental study on the influence of solution subcooling and wall superheat on sensible and evaporative heat transfer in a falling-film heat exchanger using of coated tubes (plain and porous). It was observed that the enhancement of the porous layer coated tubes was most pronounced when evaporation dominates, i.e., low solution Reynolds number, low subcooling, and high wall superheat. Fig. 8(a)–(c) illustrates the Scanning Electron Microscope (SEM) micrographs of the samples.

3.6. Horizontal smooth tube bundles

The major problem with spray evaporators is non-uniform distribution of the feed ammonia as a film outside the tubes. The importance of uniform feed distribution cannot be overemphasized. To maintain a continuous liquid film, the feed liquid must be uniformly distributed around the periphery of each tube, and the flow to each tube must be uniform [2,52,74]. They proved the fact that the coupled nature of this phenomenon renders the optimization of this system strictly for the purpose of evaporation to be extremely complex. In order to mitigate this problem, it is best to disperse a little subcooling, which increases the sensible heat transfer from the upstream tube rows, and maintain the fully-wetted thin-film evaporation conditions on the bottom most rows. The results from a saline–water spray evaporator demonstrated a decrease of 30% in heat transfer coefficients between the top and bottom tube rows [21], due to non-uniformly distributed liquid around the periphery of the tube. The proposed pattern is called falling-film mode, and might be crucial to heat transfer. Li and Kottke [32] performed an experimental study on the local heat transfer coefficients at the outer surface of tubes in shell-and-tube heat exchangers with the staggered tube arrangement. The results showed that the heat transfer was not homogeneously distributed over the tube's surfaces. Thome [75] observed the liquid flow on a row of tubes for two different film flow rates, including flow contraction and intertube flow modes, as seen in Fig. 9. This flow contraction was also observed and described by Fujita and Tsutsui [76], and their results for the topmost tube demonstrated 10–20% lower heat transfer coefficients than the other four tubes arrayed

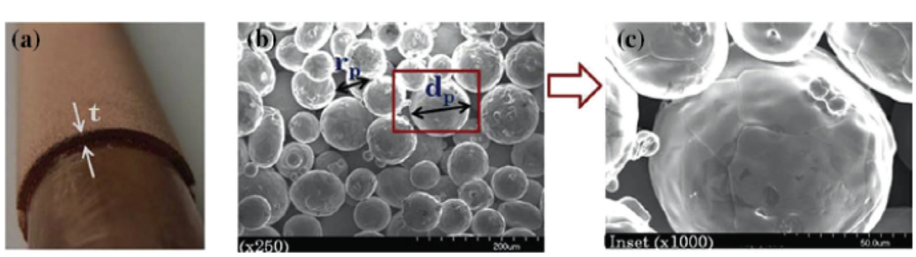

Fig. 8. (a) Photo of the porous-layer coating bonded to the plain tube, (b) 250× magnified SEM image of the porous coating and (c) 1000× magnified SEM image of the inset [73].

Please cite this article in press as: A.M. Abed, et al., The role of enhancement techniques on heat and mass transfer characteristics of shell and tube spray evaporator: a detailed review, Applied Thermal Engineering (2014), http://dx.doi.org/10.1016/j.applthermaleng.2014.10.020

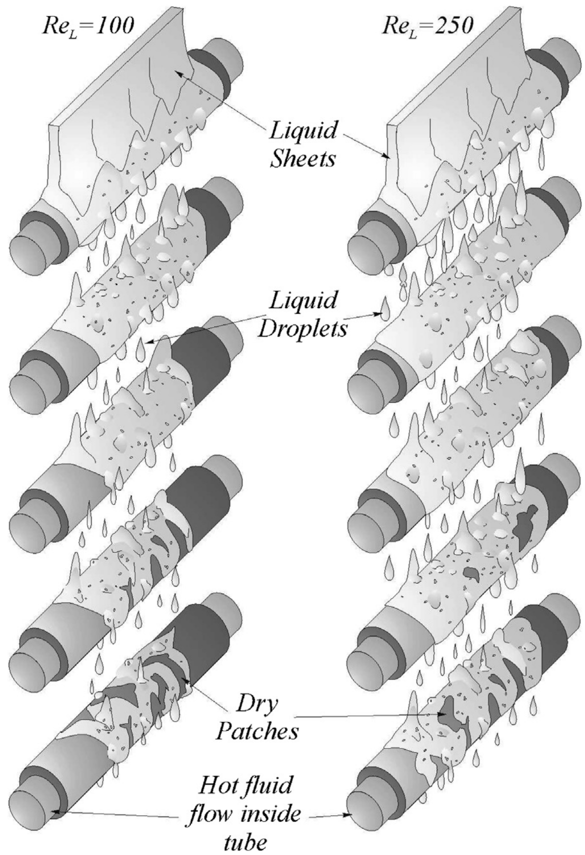

Fig. 9. Schematic of liquid film breakdown from Ref. [75].

below it. Moreover, the liquid moving through the tubes does so in many forms, such as drops, columns, or sheets, as shown in Fig. 10, and depending on the flow rate of the liquid, the physical properties of the liquid, and the separation of the tubes. At lower flow rates, as shown in Fig. 10(a), the liquid flows in the form of drops from one tube to another. When the flow rate is increased as shown in Fig. 10(b,c), the pattern is converted to circular jets or a continuous sheet. To study the phenomena of dry-out, entrainment, and the transport properties in the droplet regime, it is necessary to determine the dimensions of the drops, the distance between them, and the size of the frequency. The flow patterns observed in falling-film heat exchangers have been idealized and described by Mitrovic [77]. Ruan et al. [78] analyzed the influence of countercurrent gas flow and liquid feeding length on falling-film mode transitions for a liquid flowing over horizontal tubes. Their results proved that the influence on mode transition relies on the properties of the fluids, and can be framed in the context of unsteadiness and film thickness. Refs. [79,80] proposed a more intricate classification of flow patterns for transitional modes in a quiescent setting, and generalized a flow pattern map that predicts flow modes, shown in Fig. 11. In solar desalination units, Zheng et al. [81] studied the mechanism of both falling film evaporation and condensation. It was surmised that falling film enhances both the process of mass and heat transfers, which prompted the design of a set of highly effective, small, and compact version of the unit. Negeed and Awad [82,83] analyzed the influence of the tube's configuration and the operating conditions on the evaporation rates of a horizontal tube bundle. The results showed that both evaporation rates and Nusselt numbers increases by increasing tube surface temperature, increasing tube outer diameter, decreasing both the evaporation pressure and the inlet liquid subcooling.

3.7. Finned and enhanced tube bundle

Due to the fact that enhanced tubes are for tube bundles, it is imperative to be aware of whether the data from tube bundles will significantly differ from its single tube counterparts. Pospisil et al. [84] presented an experimental study on the backsplash characteristic of the liquid film on a wetted tube bundle with a structured surface in the atmospheric pressure. Different surface structures of the tubes were tested, namely smooth tubes, sand dressed tubes, tubes with ribbing, single, and double grooved tubes. Chang [85] conducted an experimental study on the spray using R-141b as a coolant on horizontal low-finned tube bundle, with a triangular-pitch and a fin count of 1000 fins/m. Fig. 12 shows the heat transfer performance of the low-finned tubes in the tube bundle when the liquid catchers are attached. Yang and Wang [86] numerically and experimentally analyzed the performance of the horizontal heat transfer tube bundles in falling film evaporators with an HFC-134a liquid trickling distribution system. The tubes Turbo-B, Turbo-BII and Turbo-EHP type were utilized for simulation. The Turbo-EHP demonstrated superior heat transfer performance compared to the plain, Turbo-B, and Turbo-BII tubes. Moreover, the total heat transfer rate of the Turbo-EHP tube is 62.6% higher than that of its plain tube in falling film evaporators counterpart. Li et al. [87] studied the heat transfer characteristics of falling film evaporation on horizontal tube arrays, and their results showed that tubes with both enhanced outer and inner surfaces provides high heat flux. Furthermore, it is also observed that the increase in Reynolds number decreases the heat transfer enhancement ratio of the falling film's evaporation.

Li et al. [88,89] performed an experimental study on falling film evaporation of water on 6-row horizontal enhanced tube bundles

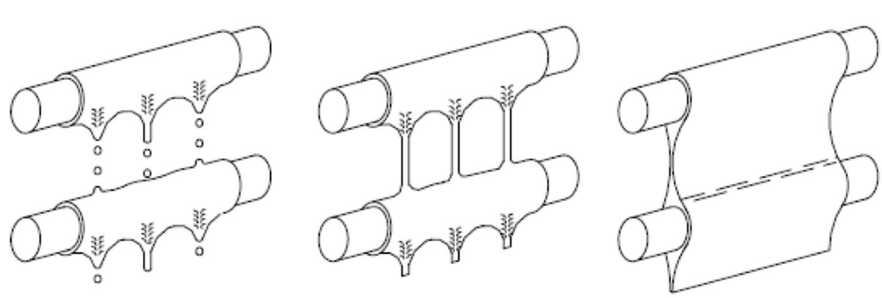

Fig. 10. Possible flow patterns of the liquid falling from one tube to another (Mitrovic 1986): (a) droplet mode, (b) the jet mode liquid leaving the tube as a continuous column; (c) sheet mode [76].

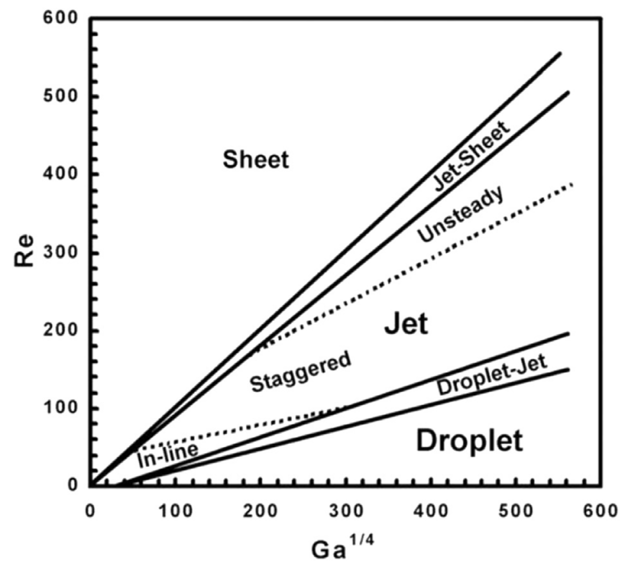

Fig. 11. The falling-film modes between horizontal tubes and flow regime map [79,80].

in a vacuum condition. Turbo-CAB (19 fpi and 26 fpi), Korodense, and smooth tubes were tested in a range of film Reynolds number from about 10 to 110. It was observed that the tubes with enhanced inner surface provide better heat transfer performance. Turbo-CAB tubes have the best heat transfer enhancement of falling film evaporation in both regimes, but Korodense tubes' overall performances were better when the tubes were fully wet. Correlations were obtained to predict the heat transfer coefficients and the heat transfer enhancement ratios of the enhanced tubes, with errors of less than ±30%.

$$Nu_{\text{o.e.wet}} = 7.42\, R_e^{-0.679} B_O^{-0.235} \left\{ \begin{array}{c} R_e > 54,\ \text{CAB} - 19\ \text{fpi} \\ R_e > 43,\ \text{CAB} - 26\ \text{fpi} \\ R_e > 65,\ \text{Korodense} \end{array} \right\} \qquad (2)$$

$$Nu_{\text{o.e.dry}} = 4.86 \times 10^{-3} R_e^{1.071} B_O^{-0.659} \left\{ \begin{array}{c} R_e > 24,\ \text{CAB} - 19\ \text{fpi} \\ R_e > 30,\ \text{CAB} - 26\ \text{fpi} \\ R_e > 43,\ \text{Korodense} \end{array} \right\} \qquad (3)$$

Christians and Thome [61,62] investigated the falling-film evaporation of a single tube row bundle and a three-row tube bundle with the express purpose of determining the local heat transfer coefficients. Four types of tubes were tested: a plain tube, an enhanced condensing tube (Gewa-C+LW, Wieland Werke, Ulm, Germany), and two enhanced boiling tubes (Turbo-EDE2, Wolverine, Hunstville, Alabama, USA; Gewa-B4, Wieland Werke, Ulm, Germany). Two refrigerants, R134a and R236fa, were tested as well. In the setting of pool boiling, the tubes performed in a superior manner compared to the tubes tested by Roques [90]and Habert [91], and demonstrated minimal dependence on the applied heat flux. The level of degradation was reduced when the test was conducted in falling-film settings.

3.8. The effect of liquid feeder configuration

In the case of convective heat transfer, the configuration of the liquid feeder might be capable of increasing the coefficient of heat transfer via the increase of convective effects that are linked to liquid impingement on a tube's surface. To improve conventional methods, different strategies are available in literature, for example, Chang and Chiou [18] conducted an experimental study on the spray using R-141b as a coolant on a horizontal staggered tube bundle. It was found that the heat transfer performance for spray cooling with a liquid film collector was much better than the pool boiling. Fig. 13 shows the differences of the overall heat transfer coefficients with and without liquid collectors under the same spray rate. Tatara and Payvar [15] introduced some liquid spray and drip boiling into the bundle for low pressure refrigerants. The placement of a distributor plate is important, as it was shown that putting it under a bundle improves heat transfer, and this is especially poignant in the case of lower vapor mass fluxes. Feeder heights can also affect heat transfers via the modification of the flow mode or by increasing the impingement velocity. Increasing the feeder height will also result

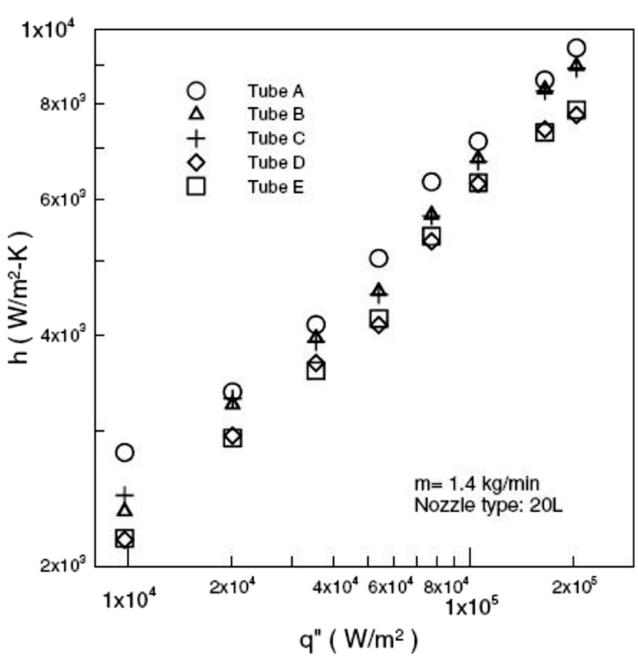

Fig. 12. Heat transfer performance of individual low-finned tubes with [85].

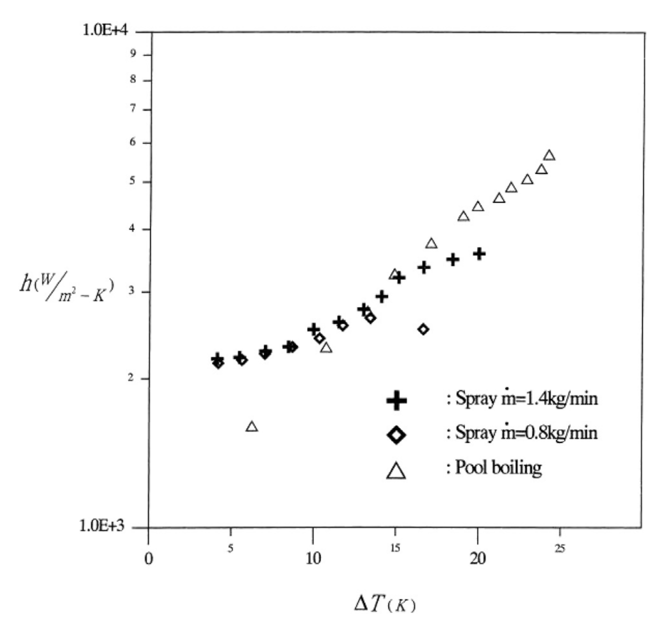

Fig. 13. Comparison of overall heat transfer (with and without liquid collector) [18].

in superior spray distribution [50]. From Negeed and Awad [82,83], it was shown that the construction of water collectors adjacent to the bottom-heated tubes improves the rate of evaporation. Chang [85] proposed a liquid catcher modification that enhances the performance of shell-and-tube heat exchangers. Fig. 14 shows the liquid catchers collecting liquid films. The work in Refs. [86,92] utilized a distributor as a designated tool that will uniformly disperse the refrigerant on the bundle equally, as shown in Fig. 15. The results also proved that the skewed distribution of refrigerant flow influences the performance of falling-film evaporators. In non-boiling settings, the distance between the spray and a hot surface is vital towards cooling improvements [27,28].

3.9. Tube passes arrangements

The arrangements of the tube are influential vis-à-vis the performance of evaporators. Multiple arrangements results in varying effect on the overall performance of heat transfer [16,21], where it was seen that the square-pitch bundle almost always results in higher spray evaporation coefficients as opposed to triangular-pitch bundle at a low saturation temperatures, as seen in Fig. 16. From the results obtained by Yang and Wang [86], it was found that the tube arrangement affects the heat transfer coefficients and the dry-out area, as shown in Fig. 17.

4. Effect of pressure drop and vapor fraction

In any heat exchanger, not only a higher overall heat transfer coefficient is desirable, but a small pressure drop is also expected in order to reduce pumping power. Designing a heat exchanger requires balancing factors between thermal design and pressure drops. Estimating the loss of pressure for fluids in a tube is relatively simple, but it gets more complicated for fluids in shell-side flows. In the effort to compute pressure drops across bundle tubes and window sections, actual flow patterns have been taken into consideration [93,94]. The total pressure drop of a fluid is due to the variation of kinetic and potential energy of the fluid, and that is due to the friction on the walls of the flow channel. Thus, the total pressure drop ΔP_{total} is calculated from Ref. [75]:

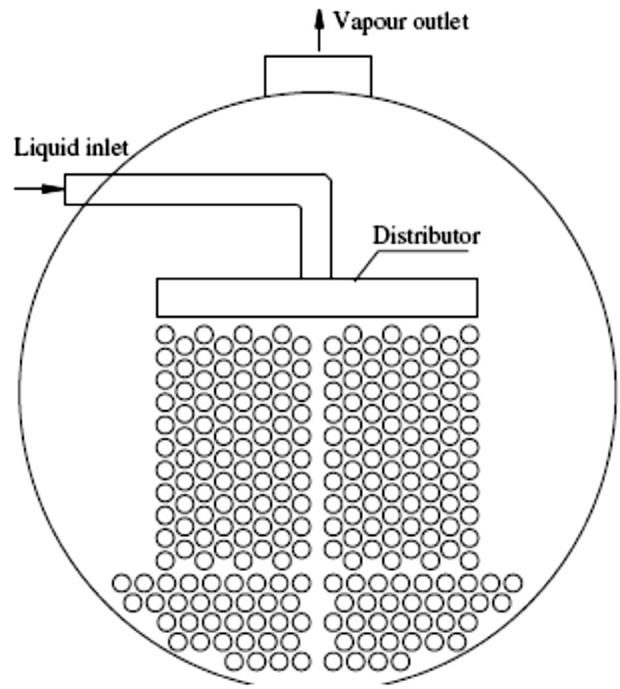

Fig. 15. Uniformly distribute on the tube bundle [86].

$$\Delta P_{total} = \Delta P_{static} + \Delta P_{mom} + \Delta P_{frict} \tag{4}$$

For a horizontal tube, there is no change in the static head, i.e. $H = 0$ so $\Delta P_{static} = 0$. The momentum pressure drop reflects the change in kinetic energy of the flow. The separated flow model considers the two phases to be artificially separated into two streams, each flowing in its own respective pipe. The areas of the two pipes are proportional to the void's fraction. The momentum pressure drop is calculable by the input of the inlet and outlet vapor qualities. When measuring two-phase pressure drops for evaporation in horizontal tubes, for instance, the frictional pressure drop is

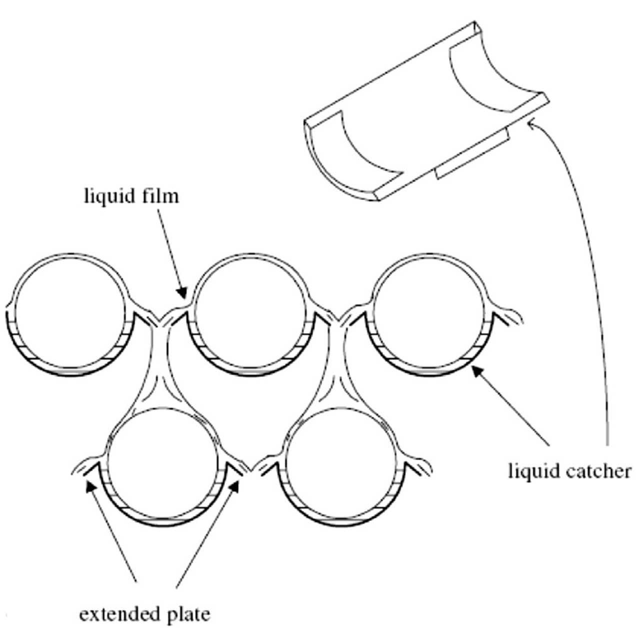

Fig. 14. Liquid film distribution with liquid catchers [85].

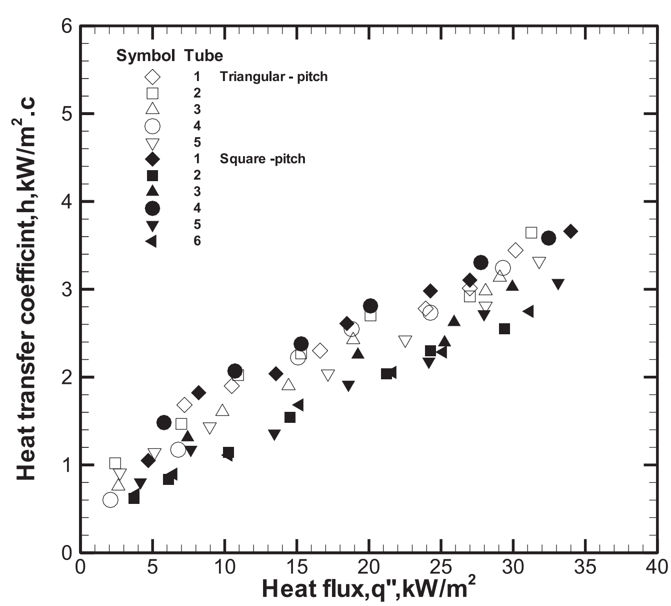

Fig. 16. Comparison between the square-pitch and triangular-pitch bundles at nozzle height of 5.08 cm. Ammonia at $T_{sat} = 10$ °C, $d = 0.75$ inch, pitch ratio of 1.25 and standard-angle nozzles [16].

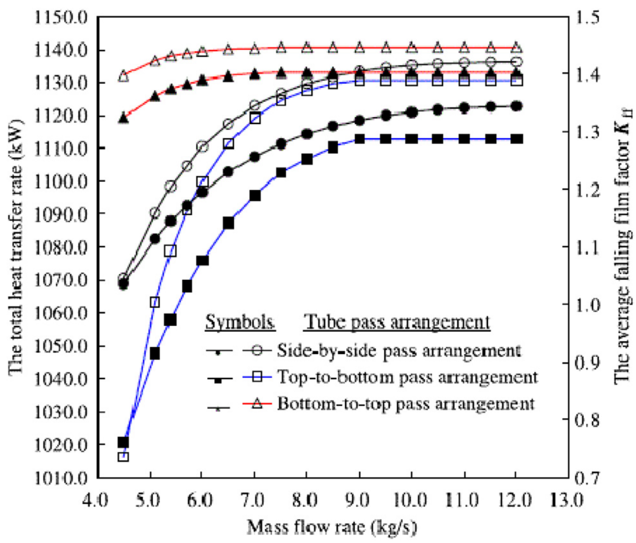

Fig. 17. Compression between different tube pass arrangement and average falling film factor (filled symbols) with refrigerant mass flow rate for Turbo-EHP [86].

obtainable by subtracting the momentum pressure drop from the measured total pressure drop, since the static pressure drop is nonexistent. Numerous methods are available for predicting the pressure drop and different parameters. Under boiling conditions, Khodabandeh [95] preformed an experimental study on the influence of heat flux, system pressure, mass flow rate, vapor fraction, on the heat transfer coefficient. It was found that the heat transfer is weakly dependent on vapor fraction, but highly dependent on heat flux and system pressures, indicating that nucleate boiling is the dominant mechanism. Refs. [96,97] measured the pressure drop for two-phase flow over the tube bundle. It was found that the frictional pressure drop was primarily a function of mass flux and vapor quality. For flat tube flow boiling [98], their results showed that the frictional pressure drop increases as the quality or mass flux increases, saturation temperature decreases, and is independent of heat flux. The frictional pressure drop also increases as the aspect ratio increases. For falling-film evaporation and condensation processes, Zheng et al. [81] pointed out the most workable processes for both heat and mass transfers. When the operating temperature is over 90 °C and the inner pressure is less than 15 kPa, the performance ratio of the unit can reach 2.35, while its yield ratio can reach about 135 kg/h. Experimental results of Xu et al. [99] for an adiabatic, two-phase vertical up and down flow of air–water mixtures across a horizontal tube bundle showed the effect of void fraction and two-phase pressure drops on the flow pattern. It showed a strong mass velocity effect, where for a given quality, a higher void fraction is obtained with increasing mass velocity. Assad and Lampinen [100] proposed a model of a countercurrent flow laminar falling film during evaporation. The interfacial shear stress is detrimental towards the evaporator's performance only in the case of countercurrent flow. The increase in the distance between the plates increases the cooling rate and decreases the pressure drop of vapor. Ribatski and Thome [101] provided a review related to the evolution of void fraction, two phase flow behaviors and pressure drop on the shell side of staggered and in-line tube bundle for upward, downward, and side-to-side flows for adiabatic air–water flows.

5. Summary of empirical correlations

Several correlations ware recently extended to compact evaporators, fin tubes, and binary mixtures. A correlation of $h+$ as a function of the film's Reynolds and Prandtl numbers was determined. Table 2 list falling-film evaporation heat transfer coefficient and Nusselt number from many researches along with the types of working fluids, pressures, temperature ranges, and evaporator designs.

6. Effect of enhanced fluid on heat and mass transfer

There are quite a number of works devoted to deeper understanding of phenomena and critical parameters that are related to spray cooling heat transfers. This is especially evident in literature detailing the fact that previous studies focused upon the influence of spray parameters on the cooling heat flux, and it was confirmed that the volumetric spray flux dominates heat transfer [23,24], mass flux of ejected fluid [28], droplet sizes and spray velocity [102], surface impact velocity [31,103], and fluid temperatures [92,104]. Chen et al. [105] performed an experimental study on the effect of spray parameters (mean droplet size, droplet flux, and droplet velocity) on critical heat flux (CHF) in subcooled water spray cooling. The results showed that the droplet velocity was the most dominant effect on CHF and heat transfer coefficients.

6.1. Effect of surfactant

Ammonia–water solution is also an attractive alternative to ozone-depleting chlorofluorocarbons (CFCs) and CO_2-emitting hydrofluorocarbons (HFCs) used in conventional vapor compression systems and absorption cooling system. Numerous researchers studied the absorption process and the effect of surfactants on heat and mass transfers in absorption chillers [106–110]. The small addition of heat transfer additives causes interfacial turbulence via the Marangoni effect, leading to improved heat and mass transfer performances [111]. Kim et al. [112] showed that the addition of surfactant increases the absorption performance by a factor of 4.81. Kim et al. [108] also indicated that the addition of surfactants (2E1H, 700 ppm) reduces the size of the absorber by 63.0%, while the application of binary nanofluids (Cu, 1000 ppm) reduces it by 54.4%. Moreover, under boiling phenomena, [113,114] provided state-of-the-art knowledge of boiling phenomena with surfactants and polymeric additives. The influence of the properties of the 12 hydrocarbons and surfactants and polymeric additives on heat transfer in nucleate pool boiling, bubble dynamics, and interfacial phenomena is taken into account by the heat transfer coefficient. The effect of different surfactant additions on heat transfer in spray cooling during evaporation has been investigated extensively in both analytical and experimental aspects [26,115,116]. Their results showed that the addition of a surfactant to water droplet reduces surface tension and increases its spreading on a solid surface. The results from Nordgrent and Setterwall [117] showed that the concentration of surfactant plays a key role in influencing surfactants with regards to the behavior of falling liquid films. Cheng et al. [118] studied heat transfer enhancement via the addition of high-alcohol surfactant (HAS) and dissolving salt additive (DSA) in spray cooling. It showed that both HAS and DSA could significantly enhance the heat transfer of water spray cooling at a suitable concentration and the HAS, especially 2-ethyl-hexanol. Recently, Yang et al. [119] conducted an experimental and theoretical study of the influence of surfactant on the preparation and stability of ammonia–water nanofluids.

6.2. Prospects of nanofluid

Spray cooling was determined to be an effective method of cooling heated surfaces. Basically, spray cooling involves the evaporation of impinging jets of droplets onto a heated surface,

Table 2
A survey of available of heat transfer correlation for falling film evaporator.

Ref. no.	Eq. no.	Correlation	Data bank	Comments
Zeng et al. [16]	5	$N = 0.0678\, Re^{0.049}\, Pr^{0.296} (p_{\mathrm{sat}}/p_{\mathrm{crit}})^{0.456} \left(\frac{qD}{(T_{\mathrm{crit}}-T_{\mathrm{sat}})k}\right)^{0.704}$	Ammonia, 3-2-3 triangular-pitch	
Zeng et al. [21]	6	$Nu = 0.0495\, Re^{-0.00399}\, Pr (p_{\mathrm{sat}}/p_{\mathrm{crit}})^{0.261} \left(\frac{qD}{(T_{\mathrm{crit}}-T_{\mathrm{sat}})k}\right)^{0.722}$	Ammonia, 3 by 3 square-pitch	
Shahzad et al. [6]	7	$h_{\mathrm{evaporation}} = 0.277 \left[\frac{h_{fg}\cdot g\cdot D^2\cdot \rho_1^2}{\nabla t^2\cdot \mu_1}\right]^{-0.333} (Re_\Gamma)^{-2.11} (P_r)^{4.55} \left(\frac{\bar{\delta}}{D}\right)^{-0.422\nabla t^{0.503}}$ $\left[\left[2\exp\left(\frac{S}{S_o}\right)-1\right]^{-0.41} \left(\frac{T_{\mathrm{sat}}}{T_{\mathrm{ref}}}\right)^{14.7}\right] + \left[0.885\left(\frac{q}{\Delta T}\right)^{1} \left(\frac{V_g}{V_{\mathrm{ref}}}\right)^{-0.34}\right]$	For seawater salinity. This correlation captures both film surface evap. and bubble agitation effects	
Armbruster and Mitrovic [45]	8	$Nu_i = 0.948 \frac{Re_L Pr_L}{2\, Ga^{\frac{1}{3}}} \left(1-\exp\left(-2\frac{Ga^{\frac{1}{3}} Nu_m}{Re_L Pr_L}\right)\right) \left(\frac{s}{d}\right)^m$ $Nu_m = 0.938\, Re_L^{1/9}\, Pr^{1/3}\, Ga^{-1/9}$	Water, smooth, unheated tubes (diameter 19.5 mm)	
Prost et al. [49]	9	$h^+ = 1.6636\, Re_L^{-0.2648}\, Pr_L^{0.1592}$		$15 < Re < 3000$, $2.5 < Pr < 200$
Zeng et al. [57]	10	$Nu = 0.0568\, Re^{-0.0058}\, Pr (p_{\mathrm{sat}}/p_{\mathrm{crit}})^{0.323} \left(\frac{qD}{(T_{\mathrm{crit}}-T_{\mathrm{sat}})k}\right)^{1.034}$	Ammonia, single 1575 (fins/m) tube	$-23 < T_{\mathrm{sa}} < 10$
Christians and Thome [61]	11	$\frac{h_{\mathrm{plateau}\ D_o}}{k_l} = 9.623{*}10^4 \left(\frac{D_o q_o^2}{h_{lv}^{\frac{5}{2}} \mu_{\mathrm{ref}} (\rho l-\rho v)}\right)^{0.0328} (G_{t-s}^{1.2449})$	R134a and R236fa for enhancement tube	Nucleate pool boiling
Putdm et al. [63]	12	$h_{\mathrm{sm}} = 0.295 \frac{k}{d} (Re_d)^{0.63} (Pr)^{0.36}$ $h_{Pr_o}/h_{\mathrm{sm}} = 0.53 (Re_\delta)^{0.11} (b/z)\cdot \exp[-0.23(b\_z)]$ To take into account the influences of fin pitch in the range of 3.0–11.8 mm. $h_{Pr}/h_{Pr_o} = 1.33 (S/S_o)^{0.45} \exp[-0.31(S/S_o)]$	For cross flow over the in-line tube bundles. For the whole range of $2 \le b/z \le 6$ profile geometry (1.4 mm $< b <$ 4.0 mm; 0.5 mm $\le z \le$ 2.0 mm; $2 < b/z < 6$; 3.0 mm $\le S \le l$ 1.8 mm)	The width-depth ratio for a groove (b/z)
Ribatski and Thome [74]	13	$h = 4.2{*}10^3 Pr^{0.22} q_{\mathrm{wet}}^{0.38} M^{-0.5} Ra^{0.2} (0.0024\, Re_{\mathrm{top}}^{0.91}) + h_{\mathrm{dry}} (1-(0.0024\, Re_{\mathrm{top}}^{0.91}))$ $Re = 6.93{*}10^5 \left(\frac{q_o}{(\rho l-\rho v) h_{lv}^{3/2}}\right)^{0.47}$	R134a, horizontal plain tubes	Falling film with nucleate boiling
Chun and Seban [163]	14	$h_{\mathrm{film}} = 0.821 \frac{\mu_1^2}{g\cdot \rho_1^2 \cdot k_1^3}^{-0.333} (Re_\Gamma)^{-0.22}$	Pure water, 319–391 K, electrical heated single vertical tube, OD – 28.58 mm, thickness – 0.1 mm, length – 292 mm	
Sernas [164]	15	$\overline{h} = Ck_{2l} \left(\frac{g}{\nu_{2l}^2}\right)^{\frac{1}{3}} \left(\frac{4\Gamma}{\mu_{2l}}\right)^{0.24} \left(\frac{\nu_{2l}}{\alpha_{2l}}\right)^{0.66}$	Horizontal tube falling film evaporation	The parameter combinations of $d = 25$ mm, $C = 0.01925$ and when $d = 50$ mm, $C = 0.01729$
Han and Fletcher [165]	16	$h_{\mathrm{evaporation}} = 0.0028 \frac{\mu_1^2}{g\cdot \rho_1^2 \cdot k_1^2}^{-0.333} (Re_\Gamma)^{0.5} (Pr)^{0.85}$	Pure water, 322–400 K, Electrical heated single horizontal tube, OD – 50.8 mm, thickness – 1.7 mm, length – 254 mm	
Shmerler and Mudawwar [166]	17	$h_E^* = 0.038 (Re_\Gamma)^{0.35} (Re_\Gamma)^{0.95}$	Pure water, electrical heated single vertical tube, OD – 25.40 mm, length – 781 mm	
Fujita and Tsutsui [167]	18	For 1st tube : $Nu = (Re_f^{-2/3} + 0.008 (Re_f^3)(Pr)^{0.25})^{1/2}$ For 2nd and 5th tube : $Nu = (Re_f^{-2/3} + 0.01 (Re_f^3)(Pr)^{0.25})^{1/2}$	Freon R-11, electrically heated five horizontal copper tubes, OD – 25 mm	
Xu et al. [46]	19	$h_{\mathrm{evaporation}} = 5.169 \times 10^{-11} \frac{h_{fg}\cdot g\cdot D^2\cdot \rho_1^2}{\nabla t^2\cdot \mu_1}^{-0.333} \left(\frac{\bar{\delta}}{D}\right)^{-0.422\nabla t^{0.503}} \left(1+\frac{\delta_{\max}-\delta_{\min}}{\delta}\right)$	De-ionized water, 323 K, horizontal copper tubes evaporator	
Chien and Tsai [168]	20	$Nu_{cv} = 0.0386 (Re_\Gamma)^{0.09} (Re_\Gamma)^{0.986}$	R245fa, 278 K & 293 K, horizontal smooth tubes	

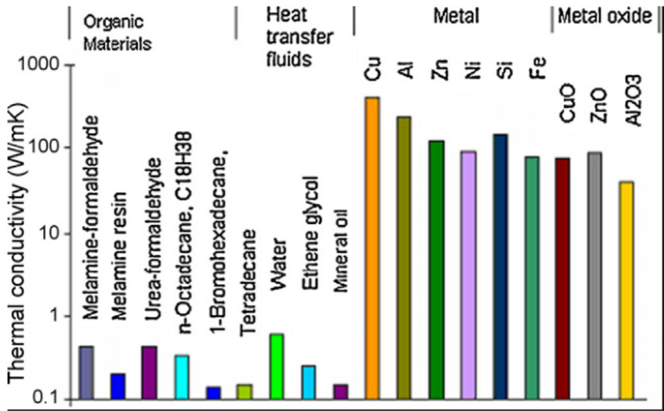

Fig. 18. Comparison of the thermal conductivity of common liquids, polymers and solids [131].

where the act of evaporation acts as a cooling medium. This is especially effective at low temperatures and also with the utilization of fluids containing nano-scale metallic particles. The integration of metallic or oxide nanoparticles to normal coolants (e.g., water, glycol and refrigerants) with the express purpose of improving both their thermal conductivities and heat transfer was done by Choi and Eastman [120]. Wang and Xu [121] proved that this integration actually improved thermal conductivities, cooling efficiencies, reduce operating costs, and also enhances heat flux. It should also be pointed out that in terms of volume fraction, the addition of these nanoparticles are rather small, but their corresponding effect is rather significant, and these improvements comes without the side effects that are common in slurries, such as clogging, erosion, sedimentation, and large increases in pressure drops. Fig. 18 shows the comparison of thermal conductivity of heat transfer fluids and nanofluids. Also, thermal conductivity enhancement of some refrigerants with nanoparticles is shown in Fig. 19. Elias et al. [122] numerically studied the effect of different nanoparticle shapes (such as cylindrical, bricks, blades, platelets, and spherical) on the performance of a shell and tube heat exchanger operating with nanofluids. Raja et al. [123] performed an experimental study on the heat transfer characteristics of Alumina/water nanofluid in an STHE, with the aid of coil insert. The overall heat transfer coefficients were increased by 17%, 29.4% and 33.5% for volume concentration percentages of 0.5, 1 and 1.5 of Alumina/water nanofluids, respectively. Lotfi et al. [124] studied the heat transfer enhancement of multi-walled carbon nanotube (MWNT)/water nanofluid in a horizontal shell and tube heat exchanger. The results showed the heat transfer enhancement in the presence of multiwalled nanotubes in comparison with the base fluid. Godson et al. [125] conducted an experimental study on the heat transfer characteristics of silver/water nanofluids in a shell and tube heat exchanger. The results showed that the maximum enhancement in convective heat transfer coefficient of 12.4% and an effectiveness of 6.14%. Farajollahi et al. [126] carried out an experimental study to investigate the heat transfer characteristics of γ-Al_2O_3/water and TiO_2/water nanofluids in a shell and tube heat exchanger under turbulent flow conditions. The experimental results for both nanofluids indicate that the heat transfer characteristics of nanofluids improved with Peclet number. Sarkar [127] studied the performance improvements of cooled shell-and-tube gas cooler, as well as CO_2 cycle using Al_2O_3, TiO_2, CuO and Cu nanofluids, and the effects of various design and operating parameters. The maximum cooling COP improvement of transcritical CO_2 cycle for $Al_2O_3 \cdot H_2O$ was 26.0%, whereas that for $TiO_2 \cdot H_2O$ was 24.4%, and for $CuO \cdot H_2O$, it was 20.7% while for $Cu \cdot H_2O$, it was 16.5%. Yang et al. [128] studied the effect of 20 types of nanoparticles mixed pairwise orthogonally with 10 types of dispersants being added in ammonia–water, respectively, to observe the dispersion stability of suspension. This begs the question of whether these fluids are suitable for falling film applications, basically, whether the change of phases in such suspensions will be beneficial or harmful vis-à-vis heat transfer. In the course of utilizing nanofluids for convective cooling, one must also keep in mind the features of its boiling nucleates. This is due to the fact that despite the nanofluids not being attracted to one another with respect to two or three phase applications, in the course of local convective heat transfer at high heat flux, the boiling limit of the nucleate pool might be exceeded. Therefore, it is imperative that the features of nanofluids under multiple conditions is explicitly known, as this will help us eschew unwanted effects such as the localization of hot spots, which will result in the significant degradation of the components that are to be cooled.

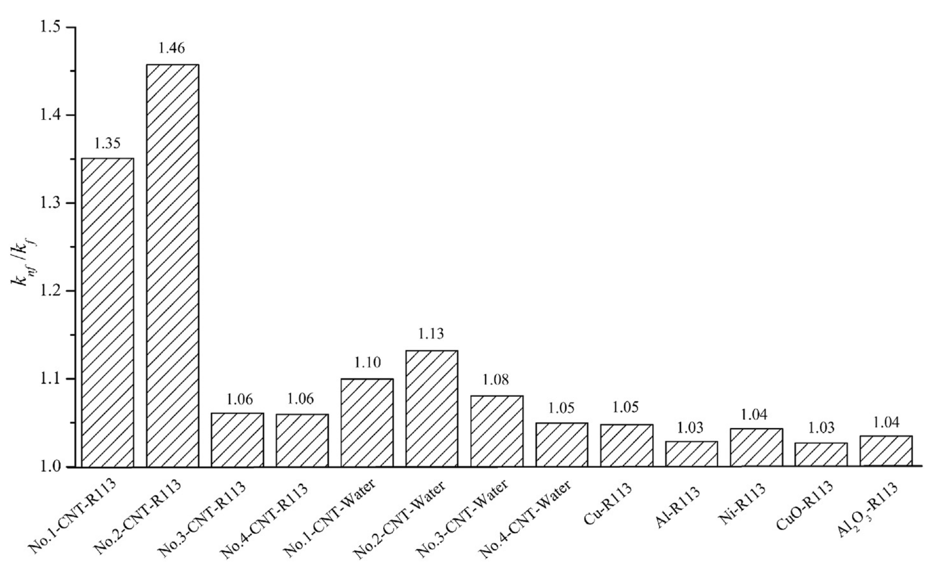

Fig. 19. Comparison of k_{nf}/k_f among CNT–R113, CNT–water and spherical-particle-R113 [132] k_{nf}, thermal conductivity of nanofluid; k_f, thermal conductivity of pure fluid.

Please cite this article in press as: A.M. Abed, et al., The role of enhancement techniques on heat and mass transfer characteristics of shell and tube spray evaporator: a detailed review, Applied Thermal Engineering (2014), http://dx.doi.org/10.1016/j.applthermaleng.2014.10.020

Table 3
Summary of studies on pool boiling of refrigerants based nanofluids.

Previous studies	Nanofluids type	Thermophysical properties	Flow type	Main results
Park and Jung [136]	(CNTs) − R123 and R134a	Ø = 1.0 vol%	Nucleate boiling	Large enhancement was up to 36.6%
Peng et al. [137]	R113 and CuO nanoparticles	⌀ = 0–0.5 wt%	Flow boiling	Maximum enhancement of heat transfer coefficient is 29.7%
Trisaksri and Wongwises [138]	TiO2–R141b	⌀ = 0.01, 0.03 and 0.05 vol%	Nucleate pool boiling	Deteriorate the heat transfer of R141b. No effect at small amount of nanoparticle
Kedzierski and Gong [139]	CuO − R134a/polyolester (RL68H) mixture	10 nm diameter at ⌀ 1.6 vol%	Pool-boiling	The nanoparticle caused heat transfer enhancement relative to the heat transfer of pure R134a/polyester
Lee et al. [140]	Al_2O_3 and CNT-NH_3/H_2O	⌀ = 0.02 vol% *dp* = 25 nm for CNT *dp* = 35 nm for Al_2O_3	Pool boiling	Absorption performance enhancement was 29% and 18% for Al_2O_3 17% and 16% for CNT
Peng et al. [141,142]	Cu and diamond − R113/(VG68) oil mixture	*dp* of 20, 50 and 80 nm nanoparticles/oil suspension from 0 to 30 wt%	Nucleate pool boiling	Heat transfer coefficient by a maximum of 23.8% for CuO and 63.4% with diamond.
Henderson et al. [143]	SiO_2 with R-134a R-134a/POE/CuO mixtures	⌀ = 0.05% and 0.5% (0.02%, 0.04%, 0.08%) vol	Pool-boiling	For SiO_2 the heat transfer coefficient decreases (up to 55%). For a 0.04% CuO the heat transfer enhancement of 52%, and with a 0.08% enhancement of 76% was measured

6.2.1. Pool boiling and two phase flow

There are quite a number of studies devoted to the characteristics of boiling and nucleate pool boiling heat transfer of water and refrigerant-based nanofluids. Defining the parameters of boiling nanofluids was first taken up by Das et al. [129], where they studied the effect of water–Al_2O_3 nanofluids in the context of boiling. The results from this study described several useful factors that are relevant to the design of cooling systems involving nanofluids, especially in situations where overheating is a risk at saturation temperatures. Table 3 summarizes studies involving nucleate pool boiling, flow boiling, and the absorption of refrigerant-based nanofluids. Recently, Saidur et al. [130] reviewed the performance of suspended nanoparticles in refrigerants and lubricating oils in refrigeration systems. The results are indicative of the fact that HFC134a and mineral oil with TiO_2 nanoparticles performs well and in a safe manner in the refrigerator, resulting in a superior performance. Nanofluids are not only capable of eradicating problems such as sedimentation, cohesion, and corrosion, which might occur in heterogeneous solid/liquid mixture with macro-or micro-sized particles, but is also capable of significantly increasing the thermal performance of the base fluids. Research involving nanofluids are divided into five groups: (1) stability analysis and experiments; (2) property measurement such as thermal conductivity and viscosity; (3) convective and boiling heat transfer; (4) mass transfer in binary nanofluids; and (5) theoretical analysis and model development.

6.2.2. Falling film flow

The effects of falling-film flow of binary nanofluids on the absorption process have been studied by several researches with the purpose of improving the performance of the absorber. Table 4 summarizes the studies of falling film and absorption of refrigerant-based nanofluid. A few data on the effect of falling film flow of binary nanofluids on heat transfer in spray cooling during evaporation is shown. Kim et al. [133] analyzed falling-film flow of binary nanofluid to determine the effect of key parameters, such as SiO_2 nanoparticles concentration on the distribution stability in the H_2O/LiBr nanofluids. It was also determined that the maximum improvements of both heat transfer and mass transfer rates

Table 4
Summary of studies on falling film absorption refrigerants based nanofluids.

Previous studies	Nanofluids type	Thermophysical properties	Flow type	Main results
Kang et al. [144]	Fe − CNT/H_2O/LiBr	⌀ = 0.01 and 0.1 wt%. *dp* = 100 nm for Fe, *dp* = 25 nm for CNT	Falling film absorption	CNT (average 2.16 for 0.01 wt% and average 2.48 for 0.1 wt%), Fe (average 1.71 for 0.01 wt% and average 1.90 for 0.1 wt%)
Jung et al. [145]	Al_2O_3/H_2O/LiBr	⌀ = 0.01, 0.05, 0.1 vol%, *dp* = 1.3 nm	Thermal conductivity measurement	Thermal conductivity of the binary nanofluids increases with the particle volume concentration and enhances by 2.2% at 0.1 vol% concentration condition
Yang et al. [146]	Al_2O_3, Fe_2O_3 and $ZnFe_2O_4$-(SDBS)/NH_3/H_2O	⌀ = 0.1–0.3 vol%	Falling film absorption	The effective absorption ratio by 70% and 50% with Fe_2O_3 and $ZnFe_2O_4$
Kim et al. [133]	SiO_2/H_2O/LiBr	⌀ = 0.01–0.005 vol%	Falling film absorption	The maximum improvements of heat transfer rate and mass transfer rate reach 46.8% and 18%, respectively
Kim et al. [108]	Surfactants with (Cu), (CuO), and (Al_2O_3)	⌀ = 0.1 vol%	Ammonia bubble absorption process	The addition of surfactants (2E1H, 700 ppm) can reduce the size of absorber up to 63.0%, while the application of binary nanofluids (Cu, 1000 ppm) can reduce it up to 54.4%.
Pang et al. [147]	(NH_3/H_2O)/Ag	⌀ = 0.005%, 0.01%, 0.02%.	Bubble absorption	55% at 0.02 wt% Ag nanoparticles
Kim et al. [148]	Surfactant and Cu, CuO and Al_2O_3 into NH_3/H_2O	*dp* = 50 nm, ⌀ = 0–0.1 vol%	Bubble behavior	Absorption performance up to 5.32 times

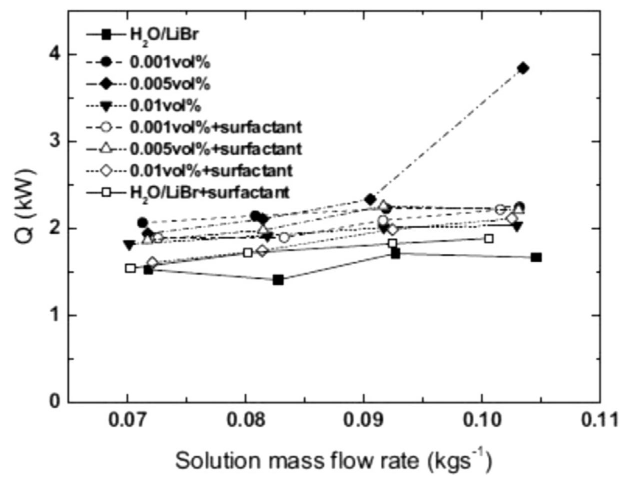

Fig. 20. Heat transfer rate versus solution mass flow rate of SiO_2 binary nanofluids for each condition [128].

reached 46.8% and 18%, respectively, when the concentration of SiO_2 nanoparticle was 0.005 vol%. Deprived of surfactants, the performance of heat transfer is enhanced via the addition of nanoparticles, as shown in Fig. 20. Chang et al. [134] analyzed the influence of particle volume fraction on spray heat transfer performance of a nanofluid that is made up of de-ionized water and Al_2O_3 particles, with a diameter of 35 nm. The particle volume fraction is defined as 0%, 0.001%, 0.025%, or 0.05%. The results showed that the high-volume-fraction nanofluids are incompatible with spray cooling. However, low-volume-fraction nanofluids (i.e., 0.001 vol%) demonstrated significant improvement in the efficiency of spray cooling, as shown in Fig. 21, due to the fact that a sizeable number of the nanoparticles ricochet from a heated surface in a direct manner or are removed by subsequent incoming droplets. Ruan and Jacobi [135] studied the characteristics of heat transfer of multiwall carbon nanotube suspensions (MWCNT nanofluids) in intertube falling-film flow. Water-based and ethylene-glycol-based nanofluids are prepared at concentrations

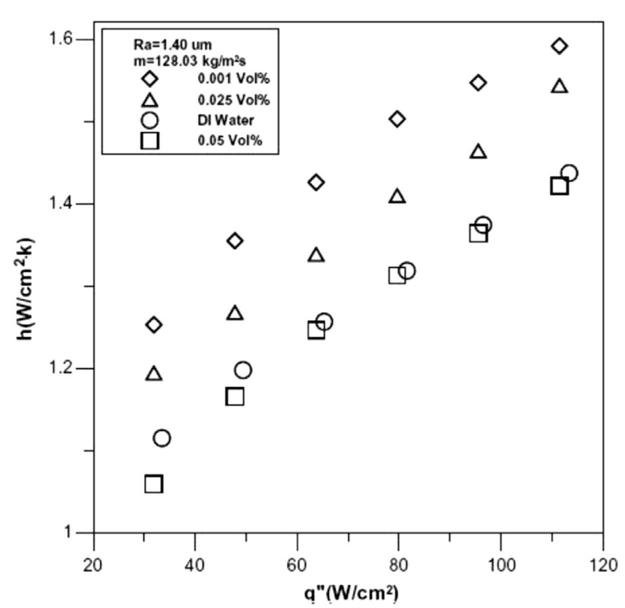

Fig. 21. Variation of heat transfer coefficient with surface heat flux as function of particle volume fraction for test surface roughness of 1.4 μm.

of 0, 0.05, 0.14 and 0.24 vol%. The results showed that the coefficient of heat transfer based on similar Reynolds number at up to 20% or higher were detected for ethylene-glycol based nanofluids. Currently, the mechanism involved in the enhancement of heat and mass transfers via falling-film flow remains murky and incomplete. There is still work to be done on the subject, especially with regards to experimental and theoretical work on many influential parameters, as this field in particular is still in its nascent stage.

7. Economic studies on cost parametric

After the mechanical design was completed, it was time for cost analysis. An overall design, in general, is the one that meets the performance requirement at a minimum cost, which includes capital cost (the costs of materials, manufacturing, testing, shipment and installation) and also operating and maintenance costs (the costs of fluid pumping powers, repair and cleaning). There are many interdependent factors that must be taken into account while designing and optimizing a heat exchanger. A low cost evaporator that would use the lowest possible heat transfer areas has already been developed [17,149,150], while others minimize the cost of STHEs [151–155]. Their results observed a reduction of total costs to up to 50% and more. Several other investigators also used strategies based on genetic optimization algorithms [156,157]. Thermoeconomic and exergy analysis in the thermal design was described by Refs. [157–159]. Due to the widespread use of this equipment, their efficient design has been analyzed from different perspective, such as exergetic analysis by Refs. [160–162] that focuses on a study of a device, based on the exergy transfer effectiveness method to evaluate factor and other relevant parameters for heat exchangers as a component. The above review anticipated knowledge of cause-effect relationships between design solutions and the cost estimation of conventional heat exchangers. The approach in the capability requires the use and building of a full-scale knowledge-based model for predicting the total cost of compact heat exchangers. This approach solves the complex design in predicting the total heat exchanger cost at any phase of the design process.

8. Conclusions

Spray cooling heat transfer is a complex phenomenon. The outstanding issues discussed in this work regarding understanding the process and technology development are very challenging. Enhanced surface tubes have been appropriately applied in multiple applications with limited success. Moreover, most authors took into account the capital cost involved in the heat transfer area and energy related costs that are connected to overcoming friction losses in fluid flow (pumping losses). The results from heat transfer showed that nanofluids are especially effective in enhancing the flow boiling heat transfer and falling-film flow of binary nanofluids of refrigerants. However, the mechanisms involved in this enhancement with nanofluids and nanoparticles are currently unknown. The inversely proportional relationship between heat transfer and the diameter of the nanoparticles also remain unclear. The challenges in particle circulation and the murky effect of falling film evaporation based on the binary nanofluid of a refrigeration system remains unaddressed. In the future, research should be directed towards the effect of the particle material, its shape, size, distribution, and concentration on the performance of spray cooling. The experimental results on the fundamental properties, such as specific heat, density, viscosity, and enthalpy of nanofluids remain minuscule in literature. There are also potential in exploring research to experimentally determine these factors. Currently, we are still without a reliable correlation between heat transfer correlations for ammonia–water falling films via the addition of nanoparticles.

References

[1] O. Lyle, The Efficient Use of Steam, H.M. Stationery Office, London, 1947.
[2] J.R. Thome, Falling film evaporation: state-of-the-art review of recent work, J. Enhanced Heat Transfer 6 (1999) 263–277.
[3] G. Ribatskia, A.M. Jacob, Falling film evaporation on horizontal tubes – a critical review, Int. J. Refrig. 28 (2005) 635–653.
[4] J. Fernández-Seara, Á.A. Pardiñas, Refrigerant falling film evaporation review: description, fluid dynamics and heat transfer, Appl. Therm. Eng. 64 (1–2) (2014) 155–171.
[5] M.C. Chyu, A.E. Bergles, Falling film evaporation on a horizontal tube, in: Multiphase Flow and Heat Transfer. ASME HTD, vol. 43, 1985, pp. 39–48.
[6] M.W. Shahzad, A. Myat, W.G. Chun, K.C. Ng, Bubble-assisted film evaporation correlation for saline water at sub-atmospheric pressures in horizontal-tube evaporator, Appl. Therm. Eng. 50 (2013) 670–676.
[7] S. Toda, Study of mist cooling (1st report: investigation of mist cooling), Heat Transfer Jpn. Res. 1 (1972) 39–50.
[8] T.G. Karayiannis, EHD boiling heat transfer enhancement of R123 and R11 on a tube bundle, Appl. Therm. Eng. 18 (1998) 809–817.
[9] S. Kabelac, H.J. De Buhr, Flow boiling of ammonia in a plain and a low finned horizontal tube, Int. J. Refrig. 24 (2001) 41–50.
[10] E. Torrella, J. Navarro-Esbrí, R. Cabello, Boiling heat-transfer coefficient variation for R407C inside horizontal tubes of a refrigerating vapour-compression plant's shell-and-tube evaporator, Appl. Energy 83 (2006) 239–252.
[11] G.H. Dooa, W.M. Dempsterb, J.M. McNaughtc, Improved prediction of shell side heat transfer in horizontal evaporative shell and tube heat exchangers, Heat Transfer Eng. 29 (2008) 999–1007.
[12] J. Zheng, M.C. Chyu, Z. Ayub, Boiling of ammonia/lubricant mixture on a horizontal enhanced tube in a flooded evaporator with inlet vapor quality, Int. J. Refrig. 31 (2008) 564–572.
[13] M.C. Chyu, J. Zheng, Z. Ayub, Bundle effect of ammonia/lubricant mixture boiling on a horizontal bundle with enhanced tubing and inlet quality, Int. J. Refrig. 32 (2009) 1876–1885.
[14] E. Gorgy, S. Eckels, Local heat transfer coefficient for pool boiling of R-134a and R-123 on smooth and enhanced tubes, Int. J. Heat Mass Transfer 55 (2012) 3021–3028.
[15] R.A. Tatara, P. Payvar, Measurement of spray boiling refrigerant coefficients in an integral – fin tube bundle segment simulating a full bundle, Int. J. Refrig. 24 (2001) 744–754.
[16] X. Zeng, M.-C. Chyu, Z.H. Ayub, Experimental investigation on ammonia spray evaporator with triangular-pitch plain-tube bundle, part II: evaporator performance, Int. J. Heat Mass Transfer 44 (2001) 2081–2092.
[17] Z.H. Ayub, M.C. Chyu, A.H. Ayub, Case study: limited charge shell and tube ammonia spray evaporator with enhanced tubes, Appl. Therm. Eng. 26 (2006) 1334–1338.
[18] T.B. Chang, J.S. Chiou, Spray evaporation heat transfer of R-141b on a horizontal tube bundle, Int. J. Heat Mass Transfer 42 (1999) 1467–1478.
[19] T.-B. Chang, C.-C. Lu, J.-C. Li, Enhancing the heat transfer performance of triangular-pitch shell and tube evaporators using an interior spray technique, Appl. Therm. Eng. 29 (2009) 2527–2533.
[20] X. Zeng, M.-C. Chyu, Z.H. Ayub, Evaporation heat transfer performance of nozzle-sprayed ammonia on a horizontal tube, ASHRAE Trans. (1995) 136–149.
[21] X. Zeng, M.-C. Chyu, Z.H. Ayub, Performance of nozzle sprayed ammonia evaporator with square-pitch plain-tube bundle, ASHRAE Trans. 103 (1997) 68–81.
[22] X. Zeng, M.-C. Chyu, Z.H. Ayub, Experimental investigation on ammonia spray evaporator with triangular-pitch plain-tube bundle, part i: tube bundle effect, Int. J. Heat Mass Transfer 44 (2001) 2299–2310.
[23] K.A. Estes, I. Mudawar, Correlation of sauter mean diameter and critical heat flux for spray cooling of small surfaces, Int. J. Heat Mass Transfer 38 (1995) 2985–2996.
[24] J.D. Bernardin, I. Mudawar, Film boiling heat transfer of droplet streams and sprays, Int. J. Heat Mass Transfer 40 (1997) 2579–2593.
[25] Z.-H. Liu, J. Wang, Study on film boiling heat transfer for water jet impinging on high temperature flat plate, Int. J. Heat Mass Transfer 44 (2001) 2475–2481.
[26] W. Jia, H.H. Qiu, Experimental investigation of droplet dynamics and heat transfer in spray cooling, Exp. Therm. Fluid Sci. 27 (2003) 829–838.
[27] A.A. Pavlova, K. Otani, M. Amitay, Active performance enhancement of spray cooling, Int. J. Heat Fluid Flow 29 (2008) 985–1000.
[28] Y. Wang, M. Liu, D. Liu, K. Xu, Y. Chen, Experimental study on the effects of spray inclination on water spray cooling performance in non-boiling regime, Exp. Therm. Fluid Sci. 34 (2010) 933–942.
[29] Y. Hou, X. Liu, J. Liu, M. Li, L. Pu, Experimental study on phase change spray cooling, Exp. Therm. Fluid Sci. 46 (2013) 84–88.
[30] J.L. Xie, Y.B. Tan, F. Duan, K. Ranjith, T.N. Wong, K.C. Toh, et al., Study of heat transfer enhancement for structured surfaces in spray cooling, Appl. Therm. Eng. 59 (2013) 464–472.
[31] Z. Zhang, J. Li, P.-X. Jiang, Experimental investigation of spray cooling on flat and enhanced surfaces, Appl. Therm. Eng. 51 (2013) 102–111.
[32] H. Li, V. Kottke, Visualization and determination of local heat transfer coefficients in shell-and-tube heat exchangers for staggered tube arrangement by mass transfer measurements, Exp. Therm. Fluid Sci. 17 (1998) 210–216.
[33] D.Y. Lee, Y. Ahn, Y. Kim, Y. Kim, Y.S. Chang, L. Nam, Experimental investigation on the drop-in performance of R407C as a substitute for R22 in a screw chiller with shell-and-tube heat exchangers, Int. J. Refrig. 25 (2002) 575–585.
[34] A. Hasan, K. Sirén, Performance investigation of plain and finned tube evaporatively cooled heat exchangers, Appl. Therm. Eng. 23 (2003) 325–340.
[35] C. Oliet, C.D. Pérez-Segarra, J. Castro, A. O, Modelling of fin-and-tube evaporators considering non-uniform in-tube heat transfer, Int. J. Therm. Sci. 49 (2010) 692–701.
[36] A. Kabul, A.K. Y, Thermal modeling of a shell and tube type evaporator with R404A, Int. J. Energy Res. 35 (2011) 633–639.
[37] J. Navarro-Esbrí, F. Molés, B. Peris, Á. Barragán-Cervera, J.M. Mendoza-Miranda, A. Mota-Babiloni, et al., Shell-and-tube evaporator model performance with different two-phase flow heat transfer correlations. Experimental analysis using R134a and R1234yf, Appl. Therm. Eng. 62 (2014) 80–89.
[38] J.S. Currie, R.E. Low, C.L. Pritchard, The performance of novel compact heat exchangers with highly extended surfaces, Appl. Therm. Eng. 16 (1996) 245–254.
[39] A. Hasan, K. Sirén, Performance investigation of plain circular and oval tube evaporatively cooled heat exchangers, Appl. Therm. Eng. 24 (2004) 777–790.
[40] X. Zeng, M.-C. Chyu, Z.H. Ayub, Experimental investigation on ammonia spray evaporator with triangular-pitch plain-tube bundle, part i: tube bundle effect, Int. J. Heat Mass Transfer 44 (2001) 2299–2310.
[41] M. Visaria, I. Mudawar, Theoretical and experimental study of the effects of spray inclination on two-phase spray cooling and critical heat flux, Int. J. Heat Mass Transfer 51 (2008) 2398–2410.
[42] E.A. Silk, J. Kim, K. Kiger, Spray cooling of enhanced surfaces: impact of structured surface geometry and spray axis inclination, Int. J. Heat Mass Transfer 49 (2006) 4910–4920.
[43] R.-L. Lin, T.-B. Chang, C.-C. Liang, Effects of spray axis incident angle on heat transfer performance of rhombus-pitch shell-and-tube interior spray evaporator, J. Mech. Sci. Technol. 26 (2012) 681–688.
[44] X. Hu, A.M. Jacobi, Departure-site spacing for liquid droplets and jets falling between horizontal circular tubes, Exp. Therm. Fluid Sci. 16 (1998) 322–331.
[45] R. Armbruster, J. Mitrovic, Evaporative cooling of a falling water film on horizontal tubes, Exp. Therm. Fluid Sci. 18 (1998) 183–194.
[46] L. Xu, M. Ge, S. Wang, Y. Wang, Heat-transfer film coefficients of falling film horizontal tube evaporators, Desalination 166 (2004) 223–230.
[47] H. Hou, Q. Bi, H. Ma, G. Wu, Distribution characteristics of falling film thickness around a horizontal tube, Desalination 285 (2012) 393–398.
[48] N. Hasan, J. Naser, Determining the thickness of liquid film in laminar condition on a rotating drum surface using CFD, Chem. Eng. Sci. 64 (2009) 919–924.
[49] J.S. Prost, M.T. González, M.J. Urbicain, Determination and correlation of heat transfer coefficients in a falling film evaporator, J. Food Eng. 73 (2006) 320–326.
[50] L. Yang, S. Shen, Experimental study of falling film evaporation heat transfer outside horizontal tubes, Desalination 220 (2008) 654–660.
[51] M.-C. Chyu, A.E. Bergles, An analytical and experimental study of falling-film evaporation on a horizontal tube, J. Heat Transfer 109 (1987).
[52] Y. Fujita, M. Tsutsui, Experimental investigation of falling film evaporation on horizontal tubes, Heat Transfer – Asian Res. 27 (1998) 609–618.
[53] A.M.I. Mohamed, Flow behavior of liquid falling film on a horizontal rotating tube, Exp. Therm. Fluid Sci. 31 (2007) 325–332.
[54] X. Wang, P.S. Hrnjak, S. Elbel, A.M. Jacobi, M. He, Flow patterns and mode transitions for falling-film on flat tubes, in: International Refrigeration and Air Conditioning, School of Mechanical Engineering: Purdue University, 2010.
[55] A.M. Jacobi, X. Wang, A thermodynamic basis for predicting falling-film mode transitions, in: International Refrigeration and Air Conditioning, 2012.
[56] F. Weise, S. Scholl, Evaporation of pure liquids with increased viscosity in a falling film evaporator, Heat Mass Transfer 45 (2007) 1037–1046.
[57] X. Zeng, M.-C. Chyu, Z.H. Ayub, Ammonia spray evaporation heat transfer performance of single low-fin and corrugated, ASHRAE Trans. 1 (1998) 325–332.
[58] O. Garcia-Valladares, J.C. González, J.I. Hernández, RBy Brown, The evaluation of a small capacity shell and tube ammonia evaporator, Appl. Therm. Eng. 23 (2003) 2151–2167.
[59] E.A. Silk, J. Kimb, K. Kiger, Spray cooling of enhanced surfaces: impact of structured surface geometry and spray axis inclination, Int. J. Heat Mass Transfer 49 (2006) 4910–4920.
[60] Z. Ayub, Current and future prospects of enhanced heat transfer in ammonia systems, Int. J. Refrig. 31 (2008) 652–657.
[61] M. Christians, J.R. Thome, Falling film evaporation on enhanced tubes, part 2: prediction methods and visualization, Int. J. Refrig. 35 (2) (2012) 313–324.
[62] M. Christians, J.R. Thome, Falling film evaporation on enhanced tubes, part 1: experimental results for pool boiling, onset-of-dryout and falling film evaporation, Int. J. Refrig. 35 (2012) 300–312.

Please cite this article in press as: A.M. Abed, et al., The role of enhancement techniques on heat and mass transfer characteristics of shell and tube spray evaporator: a detailed review, Applied Thermal Engineering (2014), http://dx.doi.org/10.1016/j.applthermaleng.2014.10.020

[63] Ju.V. Putilin, V.L. Podberezny, V.G. Rifert, Evaporation heat transfer in liquid films flowing down horizontal smooth and longitudinally profiled tubes, Desalination 105 (1996) 165–170.

[64] Z.H. Liu, J. Yi, Falling film evaporation heat transfer of water and R11falling film with roll-worked enhanced tubes bundle, Appl. Therm. Eng. 22 (2002) 83–95.

[65] Z.H. Liu, J. Yi, Falling film evaporation heat transfer of water salt mixtures from roll worked enhanced tubes and tube bundle, Appl. Therm. Eng. 22 (2002) 83–95.

[66] Z.-H. Liu, J. Yi, Enhanced evaporation heat transfer of water and R-11 falling film with the roll-worked enhanced tube bundle, Exp. Therm. Fluid Sci. 25 (2001) 447–455.

[67] N.-H. Kim, E.-J. Lee, H.-W. Byun, Evaporation heat transfer and pressure drop of R-410A in flattened smooth tubes having different aspect ratios, Int. J. Refrig. 36 (2012) 1–12.

[68] E. Forrest, E. Williamson, J. Buongiorno, L.-W. Hu, M. Rubner, R. Cohen, Augmentation of nucleate boiling heat transfer and critical heat flux using nanoparticle thin-film coatings, Int. J. Heat Mass Transfer 53 (2010) 58–67.

[69] Q. Wang, X. Ma, Z. Lan, J. Chen, T. Bai, Experimental study on mixing effect of falling film on coated division tube by thermal tracing technique, Exp. Therm. Fluid Sci. 38 (2012) 165–170.

[70] S. Lee, B. Köroğlu, C. Park, Experimental investigation of capillary-assisted solution wetting and heat transfer using a micro-scale, porous-layer coating on horizontal-tube, falling-film heat exchanger, Int. J. Refrig. 35 (2012) 1176–1187.

[71] B. Köroğlu, K.S. Lee, C. Park, Nano/micro-scale surface modifications using copper oxidation for enhancement of surface wetting and falling-film heat transfer, Int. J. Heat Mass Transfer 62 (2013) 794–804.

[72] B. Köroğlu, N. Bogan, C. Park, Effect of tube row on heat transfer and surface wetting of micro-scale porous-layer coated, horizontal-tube, falling-film evaporator, J. Heat Transfer 135 (2013) 041802.

[73] N. Bogan, C. Park, Influences of solution subcooling, wall superheat and porous-layer coating on heat transfer in a horizontal-tube, falling-film heat exchanger, Int. J. Heat Mass Transfer 68 (2014) 141–150.

[74] G. Ribatski, J.R. Thome, Experimental study on the onset of local dryout in an evaporating falling film on horizontal plain tubes, Exp. Therm. Fluid Sci. 31 (2007) 483–493.

[75] J.R. Thome, Engineering Databook III, 2006. http://www.wlv.com/products/databook/db3DataBookIII.pdf.

[76] Y. Fujita, M. Tsutsui, Evaporation heat transfer of falling films on horizontal tubes (3rd report, heat transfer of tube array), Nippon Kikai Gakkai Ronbunshu, B Hen/Trans. Jpn. Soc. Mech. Eng. Part B 63 (1997) 1701–1706.

[77] J. Mitrovic, Influence of tube spacing and flow rate on heat transfer from a horizontal tube to a falling liquid film, in: Proceedings of the Eighth International Heat Transfer Conference, San Francisco, 1986, pp. 1949–1956.

[78] B. Ruan, A.M. Jacobi, L. Li, Effects of a countercurrent gas flow on falling-film mode transitions between horizontal tubes, Exp. Therm. Fluid Sci. 33 (2009) 1216–1225.

[79] X. Hu, A.M. Jacobi, The intertube falling film 2. Mode effects on sensible heat transfer to a falling liquid film, J. Heat Transfer – Trans. ASME HTD 118 (1996) 626–633.

[80] X. Hu, A.M. Jacobi, The intertube falling film 1. Flow characteristics, mode transitions, and hysteresis, J. Heat Transfer – Trans. ASME 118 (1996) 616–625.

[81] H. Zheng, K. He, Y. Yang, Z. Chen, H. Li, Study on a multi-effects regeneration and integral-type solar desalination unit with falling film evaporation and condensation processes, Sol. Energy 80 (2006) 1189–1198.

[82] E.-S.R. Negeed, M.M. Awad, Experimental study of falling film evaporation on horizontal tube bundle for a desalination unit, Int. J. Nucl. Desalination 4 (2010) 1–17.

[83] M. Awad, E.-S.R. Negeed, Heat transfer enhancement of falling film evaporation on a horizontal tube bundle, Int. J. Nucl. Desalination 3 (2009) 283–300.

[84] J. Pospisil, L. Chroboczek, Z. Fortelny, P. Charvat, Falling film heat exchange and backsplash on horizontal tube bundles, Int. J. Energy 3 (2009).

[85] T.-B. Chang, Effects of nozzle configuration on a shell-and-tube spray evaporator with liquid catcher, Appl. Therm. Eng. 26 (2006) 814–823.

[86] L. Yang, W. Wang, The heat transfer performance of horizontal tube bundles in large falling film evaporators, Int. J. Refrig. 34 (2011) 303–316.

[87] W. Li, X.-Y. Wu, Z. Luo, S.-C. Yao, J.-L. Xu, Heat transfer characteristics of falling film evaporation on horizontal tube arrays, Int. J. Heat Mass Transfer 54 (2011) 1986–1993.

[88] W. Li, X.-Y. Wu, Z. Luo, R.L. Web, Falling water film evaporation on newly-designed enhanced tube bundles, Int. J. Heat Mass Transfer 54 (2011) 2990–2997.

[89] W. Li, X. Wu, Z. Luo, Falling Film Evaporation of Water on Horizontal Configured Tube Bundles, Washington, DC, 2010, pp. 495–502.

[90] J.F. Roques, Falling Film Evaporation on a Single Tube and on a Tube Bundle, Laboratory of Heat and Mass Transfer, Lausanne, Switzerland, 2004.

[91] M. Habert, Falling Film Evaporation on a Tube Bundle with Plain and Enhanced Tubes, Laboratory of Heat and Mass Transfer, Lausanne, Switzerland, 2009.

[92] K. Bourouni, R. Martin, L. Tadrist, H. Tadrist, Modelling of heat and mass transfer in a horizontal-tube falling-film evaporator for water desalination, Desalination 116 (1998) 165–183.

[93] U.C. Kapale, S. Chand, Modeling for shell-side pressure drop for liquid flow in shell-and-tube heat exchanger, Int. J. Heat Mass Transfer 49 (2006) 601–610.

[94] R. Hosseini, A. Hosseini-Ghaffar, M. Soltani, Experimental determination of shell side heat transfer coefficient and pressure drop for an oil cooler shell-and-tube heat exchanger with three different tube bundles, Appl. Therm. Eng. 27 (2007) 1001–1008.

[95] R. Khodabandeh, Heat transfer in the evaporator of an advanced two-phase thermosyphon loop, Int. J. Refrig. 28 (2005) 190–202.

[96] E. Van Rooyen, J.R. Thome, Pressure drop data and prediction method for enhanced external boiling tube bundles with R-134a and R-236fa, Int. J. Refrig. 36 (2013) 1669–1680.

[97] R. Dowlati, A.M.C. Chan, M. Kawaji, Two-phase crossflow and boiling heat transfer in horizontal tube bundles, J. Heat Transfer 118 (2007) 8.

[98] N.-H. Kim, E.-J. Lee, H.-W. Byun, Evaporation heat transfer and pressure drop of R-410A in flattened smooth tubes having different aspect ratios, Int. J. Refrig. 36 (2013) 363–374.

[99] G.P. Xu, C.P. Tso, K.W. Tou, Hydrodynamics of two-phase flow in vertical up and down-flow across a horizontal tube bundle, Int. J. Multiph. Flow 24 (1998) 1317–1342.

[100] M.E.H. Assad, M.J. Lampinen, Mathematical modeling of falling liquid film evaporation process, Int. J. Refrig. 25 (2002) 985–991.

[101] G. Ribatski, J.R. Thome, Dynamic of two phase flow across horizontal tube bundles – a review, in: Proceedings of 10th Brazilian Congress of Thermal Sciences and Engineering (ENCIT-2004), Rio de Janeiro, Nov. 29–Dec. 3, 2004, pp. 122–131.

[102] F.S.K. Warnakulasuriya, W.M. Worek, Drop formation of swirl-jet nozzles with high viscous solution in vacuum-new absorbent in spray absorption refrigeration, Int. J. Heat Mass Transfer 51 (2008) 3362–3368.

[103] Y.-Y. Li, Z.-H. Liu, Q. Wang, Experimental study on critical heat flux of steady boiling for high-velocity slot jet impinging on the stagnation zone, Int. J. Heat Mass Transfer 70 (2014) 1–9.

[104] H.Y. Kim, B.H. Kang, Effects of hydrophilic surface treatment on evaporation heat transfer at the outside wall of horizontal tubes, Appl. Therm. Eng. 23 (2003) 449–458.

[105] R.-H. Chen, L.C. Chow, J.E. Navedo, Effects of spray characteristics on critical heat flux in subcooled water spray cooling, Int. J. Heat Mass Transfer 45 (2002) 4033–4043.

[106] H. Daiguji, E. Hihara, Mechanism of absorption enhancement by surfactant, Int. J. Heat Mass Transfer 40 (1997) 1743–1752.

[107] S. Vemuri, K.J. Kim, Y.T. Kang, A study on effective use of heat transfer additives in the process of steam condensation, Int. J. Refrig. 29 (2006) 724–734.

[108] J.-K. Kim, A. Akisawa, T. Kashiwagi, Y.T. Kang, Numerical design of ammonia bubble absorber applying binary nanofluids and surfactants, Int. J. Refrig. 30 (2007) 1086–1096.

[109] J.-K. Kim, J.Y. Jung, Y.T. Kang, Absorption performance enhancement by nano-particles and chemical surfactants in binary nanofluids, Int. J. Refrig. 30 (2007) 50–57.

[110] R. Möller, K.F. Knoehe, Surfactants with NH3-H20, Int. J. Refrig. 19 (1996) 317–321.

[111] Y.T. Kanga, T. Kashiwagi, Heat transfer enhancement by Marangoni convection in the NH_3–H_2O absorption process, Int. J. Refrig. 25 (2002) 780–788.

[112] J.-K. Kim, J.Y. Jung, J.H. Kim, M.-G. Kim, T. Kashiwagi, Y.T. Kang, The effect of chemical surfactants on the absorption performance during NH_3/H_2O bubble absorption process, Int. J. Refrig. 29 (2006) 170–177.

[113] L. Cheng, D. Mewes, A. Luke, Boiling phenomena with surfactants and polymeric additives: a state-of-the-art review, Int. J. Heat Mass Transfer 50 (2007) 2744–2771.

[114] S. Kotthoff, D. Gorenflo, Pool boiling heat transfer to hydrocarbons and ammonia: a state-of-the-art review, Int. J. Refrig. 31 (2008) 573–602.

[115] S. Chandra, Md Marzo, Y.M. Qiao, P. Tartarini, Effect of liquid-solid contact angle on droplet evaporation, Fire Saf. J. 27 (1996) 141–158.

[116] Basit H. Shah, R. Darby, The effect of surfactant on evaporative heat transfer in vertical film flow, Int. J. Heat Mass Transfer 10 (1973) 1889–1903.

[117] M. Nordgrent, F. Setterwall, An experimental study of the effects of surfactant on a falling liquid film, Int. J. Refrig. 19 (1996) 310–316.

[118] W. Cheng, B. Xie, F. Han, H. Chen, An experimental investigation of heat transfer enhancement by addition of high-alcohol surfactant (HAS) and dissolving salt additive (DSA) in spray cooling, Exp. Therm. Fluid Sci. 45 (2013) 198–202.

[119] L. Yang, K. Du, X. Niu, Y. Li, Y. Zhang, An experimental and theoretical study of the influence of surfactant on the preparation and stability of ammonia–water nanofluids, Int. J. Refrig. 34 (2011) 1741–1748.

[120] S. Choi, J.A. Eastman, Enhancing thermal conductivity of fluids with nanoparticles, in: International Mechanical Engineering Congress and Exposition, 1995, pp. 99–105.

[121] X.W. Wang, X.F. Xu, Thermal conductivity of nanoparticle–fluid mixture, J. Thermophys. Heat Transfer 13 (1999) 474–480.

[122] M.M. Elias, M. Miqdad, I.M. Mahbubul, R. Saidur, M. Kamalisarvestani, M.R. Sohel, et al., Effect of nanoparticle shape on the heat transfer and thermodynamic performance of a shell and tube heat exchanger, Int. Commun. Heat Mass Transfer 44 (2013) 93–99.

[123] M. Raja, R.M. Arunachalam, S. Suresh, Experimental studies on heat transfer of alumina/water nanofluid in a shell and tube heat exchanger with wire coil insert, Int. J. Mech. Mater. Eng. 7 (2012) 16–23.

Please cite this article in press as: A.M. Abed, et al., The role of enhancement techniques on heat and mass transfer characteristics of shell and tube spray evaporator: a detailed review, Applied Thermal Engineering (2014), http://dx.doi.org/10.1016/j.applthermaleng.2014.10.020

[124] R. Lotfi, A.M. Rashidi, A. Amrollahi, Experimental study on the heat transfer enhancement of MWNT-water nanofluid in a shell and tube heat exchanger, Int. Commun. Heat Mass Transfer 39 (2012) 108–111.
[125] L. Godson, K. Deepak, C. Enoch, B. Jefferson, B. Raja, Heat transfer characteristics of silver/water nanofluids in a shell and tube heat exchanger, Archives Civil Mech. Eng. 14 (3) (2014) 489–496.
[126] B. Farajollahi, S.G. Etemad, M. Hojjat, Heat transfer of nanofluids in a shell and tube heat exchanger, Int. J. Heat Mass Transfer 53 (2010) 12–17.
[127] J. Sarkar, Performance of nanofluid-cooled shell and tube gas cooler in transcritical CO_2 refrigeration systems, Appl. Therm. Eng. 31 (2011) 2541–2548.
[128] L. Yang, K. Du, S. Bao, Y. Wu, Investigations of selection of nanofluid applied to the ammonia absorption refrigeration system, Int. J. Refrig. 35 (2012) 2248–2260.
[129] S.K. Das, N. Putra, W. Roetzel, Pool boiling characteristics of nano-fluids, Int. J. Heat Mass Transfer 46 (2003) 851–862.
[130] R. Saidur, S.N. Kazi, M.S. Hossain, M.M. Rahman, H.A. Mohammed, A review on the performance of nanoparticles suspended with refrigerants and lubricating oils in refrigeration systems, Renew. Sustain. Energy Rev. 15 (2011) 310–323.
[131] D. Wen, G. Lin, S. Vafaei, K. Zhang, Review of nanofluids for heat transfer applications, Particuology 7 (2009) 141–150.
[132] W. Jiang, G. Ding, H. Peng, Measurement and model on thermal conductivities of carbon nanotube nanorefrigerants, Int. J. Therm. Sci. 48 (2009) 1108–1115.
[133] H. Kim, J. Jeong, Y.T. Kang, Heat and mass transfer enhancement for falling film absorption process by SiO_2 binary nanofluids, Int. J. Refrig. 35 (2012) 645–651.
[134] T.-B. Chang, S.-C. Syu, Y.-K. Yang, Effects of particle volume fraction on spray heat transfer performance of Al_2O_3–water nanofluid, Int. J. Heat Mass Transfer 55 (2012) 1014–1021.
[135] B. Ruan, A.M. Jacobi, Heat transfer characteristics of multiwall carbon nanotube suspensions (MWCNT nanofluids) in intertube falling-film flow, Int. J. Heat Mass Transfer 55 (2012) 3186–3195.
[136] K.-J. Park, D. Jung, Boiling heat transfer enhancement with carbon nanotubes for refrigerants used in building air-conditioning, Energy Build. 39 (2007) 1061–1064.
[137] H. Peng, G. Ding, W. Jiang, H. Hu, Y. Gao, Heat transfer characteristics of refrigerant-based nanofluid flow boiling inside a horizontal smooth tube, Int. J. Refrig. 32 (2009) 1259–1270.
[138] V. Trisaksri, S. Wongwises, Nucleate pool boiling heat transfer of TiO_2–R141b nanofluids, Int. J. Heat Mass Transfer 52 (2009) 1582–1588.
[139] M.A. Kedzierski, M. Gong, Effect of CuO nanolubricant on R134a pool boiling heat transfer, Int. J. Refrig. 32 (2009) 791–799.
[140] J.K. Lee, J. Koo, H. Hong, Y.T. Kang, The effects of nanoparticles on absorption heat and mass transfer performance in NH_3/H_2O binary nanofluids, Int. J. Refrig. 33 (2010) 269–275.
[141] H. Peng, G. Ding, H. Hu, W. Jiang, D. Zhuang, K. Wang, Nucleate pool boiling heat transfer characteristics of refrigerant/oil mixture with diamond nanoparticles, Int. J. Refrig. 33 (2010) 347–358.
[142] H. Peng, G. Ding, H. Hu, W. Jiang, Effect of nanoparticle size on nucleate pool boiling heat transfer of refrigerant/oil mixture with nanoparticles, Int. J. Heat Mass Transfer 54 (2011) 1839–1850.
[143] K. Henderson, Y.-G. Park, L. Liu, A.M. Jacobi, Flow-boiling heat transfer of R-134a-based nanofluids in a horizontal tube, Int. J. Heat Mass Transfer 53 (2010) 944–951.
[144] Y.T. Kang, H.J. Kim, K.I. Lee, Heat and mass transfer enhancement of binary nanofluids for H_2O/LiBr falling film absorption process, Int. J. Refrig. 31 (2008) 850–856.
[145] J.-Y. Jung, C. Cho, W.H. Lee, Y.T. Kang, Thermal conductivity measurement and characterization of binary nanofluids, Int. J. Heat Mass Transfer 54 (2011) 1728–1733.
[146] L. Yang, K. Du, X.F. Niu, B. Cheng, Y.F. Jiang, Experimental study on enhancement of ammonia–water falling film absorption by adding nanoparticles, Int. J. Refrig. 34 (2011) 640–647.
[147] C. Pang, W. Wu, W. Sheng, H. Zhang, Y.T. Kang, Mass transfer enhancement by binary nanofluids (NH_3/H_2O + Ag nanoparticles) for bubble absorption process, Int. J. Refrig. 35 (2012) 2240–2247.
[148] J.-K. Kim, J.Y. Jung, Y.T. Kang, The effect of nano-particles on the bubble absorption performance in a binary nanofluid, Int. J. Refrig. 29 (2006) 22–29.
[149] S.A. Kalogirou, Design of a new spray-type seawater evaporator, Desalination 139 (2001) 345–352.
[150] S. Sharma, G.P. Rangaiah, K.S. Cheah, Multi-objective optimization using MS excel with an application to design of a falling-film evaporator system, Food Bioprod. Process. 90 (2012) 123–134.
[151] A.V. Azad, M. Amidpour, Economic optimization of shell and tube heat exchanger based on constructal theory, Energy 36 (2011) 1087–1096.
[152] A.C. Caputo, P.M. Pelagagge, P. Salini, Heat exchanger design based on economic optimisation, Appl. Therm. Eng. 28 (2008) 1151–1159.
[153] B. Khalifeh Soltan, M. Saffar-Avval, E. Damangir, Minimizing capital and operating costs of shell and tube condensers using optimum baffle spacing, Appl. Therm. Eng. 24 (2004) 2801–2810.
[154] M. Serna-González, J.M. Ponce-Ortega, Total cost target for heat exchanger networks considering simultaneously pumping power and area effects, Appl. Therm. Eng. 31 (2011) 1964–1975.
[155] A. Hadidi, M. Hadidi, A. Nazari, A new design approach for shell-and-tube heat exchangers using imperialist competitive algorithm (ICA) from economic point of view, Energy Convers. Manag. 67 (2013) 66–74.
[156] A. Hadidi, A. Nazari, Design and economic optimization of shell-and-tube heat exchangers using biogeography-based (BBO) algorithm, Appl. Therm. Eng. 51 (2013) 1263–1272.
[157] H. Hajabdollahi, P. Ahmadi, I. Dincer, Thermoeconomic optimization of a shell and tube condenser using both genetic algorithm and particle swarm, Int. J. Refrig. 34 (2011) 1066–1076.
[158] D. Eryener, Thermoeconomic optimization of baffle spacing for shell and tube heat exchangers, Energy Convers. Manag. 47 (2006) 1478–1489.
[159] G. Tsatsaronis, Thermoeconomic analysis and optimization of energy systems, Prog. Energy Combust. Sci. 19 (1993) 227–257.
[160] S.-Y. Wu, X.-F. Yuan, Y.-R. Li, L. Xiao, Exergy transfer effectiveness on heat exchanger for finite pressure drop, Energy 32 (2007) 2110–2120.
[161] A. Gupta, S.K. Das, Second law analysis of crossflow heat exchanger in the presence of axial dispersion in one fluid, Energy 32 (2007) 664–672.
[162] J.Y. San, Second-law performance of heat exchangers for waste heat recovery, Energy 35 (2010) 1936–1945.
[163] K.R. Chun, R.A. Seban, Heat transfer to evaporating liquid films, ASME J. Heat Transfer 11 (1971) 391–396.
[164] V. Sernas, Heat transfer correlation for subcooled water films on horizontal tubes, J. Heat Transfer 101 (1979) 176–178.
[165] J.C. Han, L.S. Fletcher, Falling film evaporation and boiling in circumferential and axial grooves on horizontal tubes, Ind. Eng. Chem. Process Des. Dev. 24 (1985) 570–575.
[166] J.A. Shmerler, I. Mudawwar, Local evaporative heat transfer coefficient in turbulent free-falling liquid films, Int. J. Heat Mass Transfer 31 (1988) 731–742.
[167] Y. Fujita, M. Tsutsui, Experimental investigation of falling film evaporation on horizontal tubes, Heat Trans. Jpn. Res. 27 (1998) 609–618.
[168] L.-H. Chien, Y.-L. Tsai, An experimental study of pool boiling and falling film vaporization on horizontal tubes in R-245fa, Appl. Therm. Eng. 31 (2011) 4044–4054.

Please cite this article in press as: A.M. Abed, et al., The role of enhancement techniques on heat and mass transfer characteristics of shell and tube spray evaporator: a detailed review, Applied Thermal Engineering (2014), http://dx.doi.org/10.1016/j.applthermaleng.2014.10.020